

1 **SYNERGY BETWEEN SATELLITE OBSERVATIONS OF SOIL MOISTURE**  
2 **AND WATER STORAGE ANOMALIES FOR RUNOFF ESTIMATION**

3 Stefania Camici <sup>(1)</sup>, Gabriele Giuliani <sup>(1)</sup>, Luca Brocca <sup>(1)</sup>, Christian Massari <sup>(1)</sup>, Angelica Tarpanelli  
4 <sup>(1)</sup>, Hassan Hashemi Farahani <sup>(2)</sup>, Nico Sneeuw <sup>(2)</sup>, Marco Restano <sup>(3)</sup>, Jérôme Benveniste <sup>(4)</sup>

5 *(1) National Research Council, Research Institute for Geo-Hydrological Protection, Perugia, Italy ([s.camici@irpi.cnr.it](mailto:s.camici@irpi.cnr.it))*

6 *(2) Institute of Geodesy, University of Stuttgart, Geschwister-Scholl-Straße 24D, 70174 Stuttgart, Germany*

7 *(3) SERCO c/o ESA-ESRIN, Largo Galileo Galilei, Frascati, 00044, Italy*

8 *(4) European Space Agency, ESA-ESRIN, Largo Galileo Galilei, Frascati, 00044, Italy*

9

10

11

12

13

14

15

16

17

18

**November 2020**

19

Submitted to:

20

\* Correspondence to: Ph.D. Stefania Camici, Research Institute for Geo-Hydrological Protection, National Research Council, Via della Madonna Alta 126, 06128 Perugia, Italy. Tel: +39 0755014419 Fax: +39 0755014420 E-mail: [stefania.camici@irpi.cnr.it](mailto:stefania.camici@irpi.cnr.it).

## 21 **ABSTRACT**

22 This paper presents an innovative approach, STREAM - SaTellite based Runoff Evaluation And  
23 Mapping - to derive daily river discharge and runoff estimates from satellite soil moisture,  
24 precipitation and terrestrial water storage anomalies observations. Within a very simple model  
25 structure, the first two variables (precipitation and soil moisture) are used to estimate the quick-flow  
26 river discharge component while the terrestrial water storage anomalies are used for obtaining its  
27 complementary part, i.e., the slow-flow river discharge component. The two are then summed up to  
28 obtain river discharge and runoff estimates.

29 The method is tested over the Mississippi river basin for the period 2003-2016 by using Tropical  
30 Rainfall Measuring Mission (TRMM) Multi-satellite Precipitation Analysis (TMPA) precipitation  
31 data, European Space Agency Climate Change Initiative (ESA CCI) soil moisture data and Gravity  
32 Recovery and Climate Experiment (GRACE) terrestrial water storage data. Despite the model  
33 simplicity, relatively high-performance scores are obtained in river discharge simulations, with a  
34 Kling-Gupta efficiency index greater than 0.65 both at the outlet and over several inner stations used  
35 for model calibration highlighting the high information content of satellite observations on surface  
36 processes. Potentially useful for multiple operational and scientific applications (from flood warning  
37 systems to the understanding of water cycle), the added-value of the STREAM approach is twofold:  
38 1) a simple modelling framework, potentially suitable for global runoff monitoring, at daily time scale  
39 when forced with satellite observations only, 2) increased knowledge on the natural processes, human  
40 activities and on their interactions on the land.

41

42 Key words: satellite products, soil moisture, water storage variations, conceptual hydrological  
43 modelling, rainfall-runoff modelling, Mississippi.

## 44 1. INTRODUCTION

45 Spatial and temporal continuous river discharge monitoring is paramount for improving the  
46 understanding of the hydrological cycle, for planning human activities related to water use as well as  
47 to prevent/mitigate the losses due to extreme flood events. To accomplish these tasks, runoff and river  
48 discharge data, which represents the aggregated signal of runoff ([Fekete et al., 2012](#)), should be  
49 available at adequate spatial/temporal resolution, i.e., at basin scale (basin area larger than 10'000  
50 km<sup>2</sup>) and at monthly time step for water resources management and drought monitoring up to grid  
51 scale (few km)/(sub-) daily time step for flood prediction. The accurate continuous (in space and  
52 time) runoff and river discharge estimation at finer spatial/temporal resolution is still a big challenge  
53 for hydrologists.

54 Traditional in situ observations of river discharge, even if generally characterized by high temporal  
55 resolution (up to sub-hourly time step), typically offer little information on the spatial distribution of  
56 runoff within a watershed. Moreover, river discharge observation networks suffer from many  
57 limitations such as low station density and often incomplete temporal coverage, substantial delay in  
58 data access and large decline in monitoring capacity ([Vörösmarty et al. 2002](#)). Paradoxically, this  
59 latter issue is exacerbated in developing nations ([Crochemore et al, 2020](#)), where the knowledge of  
60 the terrestrial water dynamics deserves greater attention due to huge damages to settlements and  
61 especially the loss of human lives that occurs regularly.

62 This precarious situation has led to growing interest in finding alternative solutions, i.e., model-based  
63 or observation-based approaches, for runoff and river discharge monitoring. Model-based  
64 approaches, based on the mathematical description of the main hydrological processes (e.g., water  
65 balance models, WBMs, global hydrological models, GHMs, e.g., [Döll et al., 2003](#) or, increasing in  
66 complexity, land surface models, LSM, e.g., [Balsamo et al., 2009](#); [Schellekens et al., 2017](#)), are able  
67 to provide comprehensive information on a large number of relevant variables of the hydrological  
68 cycle including runoff and river discharge at very high temporal and spatial resolution (up to hourly

sampling and 0.05° grid scale). However, the values of simulated water balance components rely on a massive parameterization of the soil, vegetation and land parameters, which is not always realistic, and are strongly dependent on the GHM/ LSM models used, analysis periods ([Wisser et al., 2010](#)) and climate forcings selected (e.g. [Haddeland et al., 2012](#); [Gudmundsson et al., 2012a, b](#); [Prudhomme et al., 2014](#); [Müller Schmied et al., 2016](#)).

Alternatively, the observation-based approaches exploit machine learning techniques and a considerable amount of data to describe the physics of the system (i.e. hydraulic and/or hydrologic phenomena, [Solomatine and Ostfeld, 2008](#)) with only a limited number of assumptions. Besides being simpler than model-based approaches, these approaches still present some limitations. At first, as they rely on a considerable amount of data describing the modelled system's physics, the spatial/temporal extent and the uncertainty of the resulting dataset is determined by the spatial/temporal coverage and the accuracy of the forcing data (e.g., see E-RUN dataset, [Gudmundsson and Seneviratne, 2016](#); GRUN dataset, [Ghiggi et al., 2019](#); FLO1K dataset, [Barbarossa et al., 2018](#)). Additional limitations stem from the employed method to estimate runoff. Indeed, random forests such as employed in [Gudmundsson and Seneviratne, 2016](#), like other machine learning techniques, are powerful tools for data driven modeling, but they are prone to overfitting, implying that noise in the data can obscure possible signals ([Hastie et al., 2009](#)). Moreover, the influence of land parameters on continental-scale runoff dynamics is not taken into account as the underlying hypothesis is that the hydrological response of a basin exclusively depend on present and past atmospheric forcing. It is easy to understand that this assumption will only be valid in certain circumstances and might lead to problems, e.g., over complex terrain ([Orth and Seneviratne, 2015](#)) or in cases of human river flow regulation ([Ghiggi et al., 2019](#)).

Remote sensing can provide estimates of nearly all the climate variables of the global hydrological cycle including soil moisture (e.g., [Wagner et al., 2007](#); [Seneviratne et al., 2010](#)), precipitation ([Huffman et al., 2014](#)) and total terrestrial water storage (e.g., [Houborg et al., 2012](#); [Landerer and Swenson, 2012](#); [Famiglietti and Rodell, 2013](#)). It has undeniably changed and improved dramatically

95 the ability to monitor the global water cycle and, hence, runoff. By taking advantage of satellite  
96 information, some studies tried to develop methodologies able to optimally produce multivariable  
97 datasets from the fusion of in situ and satellite-based observations (e.g., [Rodell et al., 2015](#); [Zhang et](#)  
98 [al., 2018](#); [Pellet et al., 2019](#)). Other studies exploited satellite observations of hydrological variables,  
99 e.g., precipitation ([Hong et al., 2007](#)), soil moisture ([Massari et al., 2014](#)), and geodetic variables (e.g.,  
100 [Sneeuw et al., 2014](#); [Tourian et al., 2018](#)) to monitor single components of the water cycle in an  
101 independent way.

102 Although the majority of these studies provide runoff and river discharge data at basin scale and  
103 monthly time step, they deserve to be recalled here as important for the purpose of the present study.  
104 In particular, [Hong et al. \(2007\)](#) presented a first attempt to obtain an approximate but quasi-global  
105 annual streamflow dataset, by incorporating satellite precipitation data in a relatively simple rainfall-  
106 runoff simulation approach. Driven by the multiyear (1998-2006) Tropical Rainfall Measuring  
107 Mission Multi-satellite Precipitation Analysis, runoff was independently computed for each global  
108 land surface grid cell through the Natural Resources Conservation Service (NRCS) runoff curve  
109 number (CN) method ([NRCS, 1986](#)) and subsequently routed to the watershed outlet to simulate  
110 streamflow. The results, compared to the in situ observed discharge data, demonstrated the potential  
111 of using satellite precipitation data for diagnosing river discharge values both at global scale and for  
112 medium to large river basins. If, on the one hand, the work of [Hong et al. \(2007\)](#) can be considered  
113 as a pioneer study, on the other hand it presents a serious drawback within the NRCS-CN method  
114 that lacks a realistic definition of the soil moisture conditions of the catchment before flood events.  
115 This aspect is not negligible, as it is well established that soil moisture is paramount in the partitioning  
116 of precipitation into surface runoff and infiltration inside a catchment ([Brocca et al., 2008](#)). In  
117 particular, for the same rainfall amount but different values of initial soil moisture conditions,  
118 different flooding effects can occur (see e.g. [Crow et al., 2005](#); [Brocca et al., 2008](#); [Berthet et al.,](#)  
119 [2009](#); [Merz and Bloschl, 2009](#); [Tramblay et al., 2010](#)). On this line following [Brocca et al. \(2009\)](#),  
120 [Massari et al. \(2016\)](#) presented a very first attempt to estimate global streamflow data by using

121 satellite Soil Moisture Active and Passive (SMAP, Entekhabi et al., 2010) and Global Precipitation  
122 Measurement (GPM, [Huffman et al., 2019](#)) products. Although the validation was carried out by  
123 routing the monthly surface runoff only in a single basin in Central Italy, the obtained results  
124 suggested to dedicate additional efforts in this direction.

125 Among the studies that use satellite observations of hydrological variables for runoff estimation, the  
126 hydro-geodetic approaches are undoubtedly worth mentioning, see e.g., ([Sneeuw et al., 2014](#)) for a  
127 comprehensive overview or [Lorenz et al. \(2014\)](#) for an analysis of satellite-based water balance  
128 misclosures with discharge as closure term. In particular, the satellite mission Gravity Recovery And  
129 Climate Experiment (GRACE), which observed the temporal changes in the gravity field, has given  
130 a strong impetus to satellite-driven hydrology research ([Tapley et al., 2019](#)). Since temporal gravity  
131 field variations over the continents imply water storage change, GRACE was the first remote sensing  
132 system to provide observational access to deeper groundwater storage. The relation between GRACE  
133 groundwater storage change and runoff was characterized by [Riegger and Tourian \(2014\)](#), which even  
134 allowed the quantification of absolute drainable water storage over the Amazon ([Tourian et al., 2018](#)).

135 In essence the storage-runoff relation describes the gravity-driven drainage of a basin and, hence, the  
136 slow-flow processes. Due to GRACE's spatial-temporal resolution, runoff and river discharge are  
137 generally available for large basins ( $>160'000 \text{ km}^2$ ) and at monthly time step.

138 Based on the above discussion, it is clear that each approach presents strengths and limitations that  
139 enable or hamper the runoff and river discharge monitoring at finer spatial and temporal resolutions.

140 In this context, this study presents an attempt to find an alternative method to derive daily river  
141 discharge and runoff estimates at  $\frac{1}{4}$  degree spatial resolution exploiting satellite observations and the  
142 knowledge of the key mechanisms and processes that act in the formation of runoff, i.e., the role of  
143 soil moisture in determining the response of a catchment to precipitation. For that, soil moisture,  
144 precipitation and terrestrial water storage anomalies (TWSA) observations are used as input into a  
145 simple modelling framework named STREAM v1.3 (SaTellite based Runoff Evaluation And  
146 Mapping, version 1.3). Unlike classical land surface models, STREAM exploits the knowledge of the

147 system states (i.e., soil moisture and TWSA) to derive river discharge and runoff, and thus it 1) skips  
148 the modelling of the evapotranspiration fluxes which are known to be a non-negligible source of  
149 uncertainty (Long et al. 2014), 2) limits the uncertainty associated with the over-parameterization of  
150 soil and land parameters and 3) implicitly takes into account processes, mainly human-driven (e.g.,  
151 irrigation, change in the land use), that might have a large impact on the hydrological cycle and hence  
152 on runoff.

153 The detailed description of the STREAM v1.3 model is given in section 4. The collected datasets and  
154 the experimental design for the Mississippi River Basin (section 2) are described in sections 3 and 5,  
155 respectively. Results, discussion and conclusions are drawn in section 6, 7 and 8, respectively.

## 156 2. STUDY AREA

157 The STREAM v1.3 model presented here has been tested and validated over the Mississippi River  
158 basin. With a drainage area of about 3.3 million km<sup>2</sup>, the Mississippi River basin is the fourth largest  
159 watershed in the world, bordered to the West by the crest of the Rocky Mountains and to the East by  
160 the crest of the Appalachian Mountains. According to the Köppen climate classification, the climate  
161 is subtropical humid over the southern part of the basin, continental humid with hot summer over the  
162 central part, continental humid with warm summer over the eastern and norther parts, whereas a  
163 semiarid cold climate affects the western part. The average annual air temperature across the  
164 watershed ranges from 4°C in the West to 6°C in the East. On average, the watershed receives about  
165 900 mm/year of precipitation (77% as rainfall and 23% as snowfall), more concentrated in the eastern  
166 and southern portions of the basin with respect to its northern and western part (Vose et al., 2014).

167 [The river flow has a clear natural seasonality mainly controlled by spring snowmelt \(coming from](#)  
168 [the Missouri and the Upper Mississippi, the eastern and the upper part of the basin, respectively, Dyer](#)  
169 [2008\) and by heavy precipitation exceeding the soil moisture storage capacity \(mostly occurring in](#)  
170 [the eastern and southern part of the basin, Berghuijs et al., 2016\). The basin is also heavily regulated](#)  
171 [by the presence of large dams](#)~~The river flow has a clear natural seasonality mainly controlled by~~

172 ~~spring snowmelt in the mountainous areas of the basins and by heavy rainfall exceeding the soil~~  
173 ~~moisture storage capacity in the central and southern part of the basin (Berghuijs et al., 2016), but it~~  
174 ~~is also heavily regulated by the presence of about 1000 large dams~~ (Global Reservoir and Dam  
175 Database GRanD, [Lehner et al., 2011](#)) ~~most of them located on the Missouri river. In particular, the~~  
176 ~~river reach between Garrison and Gavins Point dams is the portion of the Missouri river where the~~  
177 ~~large main-channel dams have the greatest impact on river discharge providing a substantial reduction~~  
178 ~~in the annual peak floods, an increase on low flows and a reduction on the overall variability of intra-~~  
179 ~~annual discharges (Alexander et al., 2012) spread out across the basin.~~ The annual average of  
180 Mississippi river discharge at the Vicksburg outlet section is equal to  $17'500 \text{ m}^3/\text{s}$  (see Table 1).  
181 Given the variety of climate and topography across the Mississippi River basin, it is a good candidate  
182 to test the suitability of the STREAM v1.3 model for river discharge and runoff simulation.

### 183 3. DATASETS

184 The datasets used in this study include in situ observations, satellite products and model outputs. The  
185 first two datasets have been used as input data to the STREAM v1.3 model. Conversely, the model  
186 outputs are used as a benchmark to validate the performance of the STREAM v1.3 model.

#### 187 3.1 In situ Observations

188 In situ observations comprise air temperature ( $T_{\text{air}}$ ) and river discharge data ( $Q$ ).  
189 For  $T_{\text{air}}$  data the Climate Prediction Center (CPC) Global Temperature data developed by the  
190 American National Oceanic and Atmospheric Administration (NOAA) using the optimal  
191 interpolation of quality-controlled gauge records of the Global Telecommunication System (GTS)  
192 network ([Fan et al., 2008](#)) have been used. The dataset, downloadable at  
193 (<https://psl.noaa.gov/data/gridded/data.cpc.globaltemp.html>) is available on a global regular  
194  $0.5^\circ \times 0.5^\circ$  grid, and provides daily maximum ( $T_{\text{max}}$ ) and minimum ( $T_{\text{min}}$ ) air temperature data from  
195 1979 to present. The daily average air temperature data have been generated as the mean of  $T_{\text{max}}$  and  
196  $T_{\text{min}}$  of each day.

Formattato: Sottolineato

Formattato: Apice



Daily  $Q$  data over the study basins have been taken from the Global Runoff Data Center (GRDC, [https://www.bafg.de/GRDC/EN/Home/homepage\\_node.html](https://www.bafg.de/GRDC/EN/Home/homepage_node.html)). In particular, 11 gauging stations located along the main river network of the Mississippi River basin have been selected to represent the spatial distribution of runoff over the basin. The location of these gauging stations along with relevant characteristics (e.g., the upstream basin area, the mean annual river discharge and the presence of upstream dams) are summarized in Table 1. As it can be noted, mean annual river discharge ranges from 141 to 17'500 m<sup>3</sup>/s, and 3 out 11 sections are located downstream big dams (Lehner et al., 2011). In particular, Garrison (the fifth-largest earthen dam in the world), Gavins Point and Kanopolis dams located downstream section 1, 2 and 5 respectively (see Figure 3 and Table 1), are three large dams with a maximum storage of 29'383×10<sup>9</sup> m<sup>3</sup>, 0.607×10<sup>9</sup> m<sup>3</sup>, and 1.058×10<sup>9</sup> m<sup>3</sup> respectively. As it can be noted, mean annual river discharge ranges from 141 to 17'500 m<sup>3</sup>/s, and 3 out 11 sections are located downstream big dams (Lehner et al., 2011).

### 3.2 Satellite Products

Satellite products include observations of precipitation ( $P$ ), soil moisture and TWSA. The satellite  $P$  dataset used in this study is the Multi-satellite Precipitation Analysis 3B42 Version 7 (TMPA 3B42 V7) estimate produced by the National Aeronautics and Space Administration (NASA) as the 0.25°×0.25° quasi-global (50°N-S) gridded dataset. The TMPA 3B42 V7 is a gauged-corrected satellite product, with a latency period of two months after the end of the month of record, available at 3h sampling interval from 1998 to present (2020). Major details about the  $P$  dataset, downloadable from <http://pmm.nasa.gov/data-access/downloads/trmm>, can be found in [Huffman et al. \(2007\)](#). Soil moisture data have been taken from the European Space Agency Climate Change Initiative (ESA CCI) Soil Moisture project (<https://esa-soilmoisture-cci.org/>) that provides a surface soil moisture product (referred to first 2-3 centimeters of soil) continuously updated in term of spatial-temporal coverage, sensors and retrieval algorithms ([Dorigo et al., 2017](#)). In this study, the daily combined

221 ESA CCI soil moisture product v4.2 is used, that is available at global scale with a grid spacing of  
222 0.25°, for the period 1978-2016.

223 TWSA have been obtained from the Gravity Recovery And Climate Experiment (GRACE) satellite  
224 mission. Here we employ the NASA Goddard Space Flight Center (GSFC) global mascon model,  
225 i.e., Release v02.4, (Luthcke et al. 2013). It has been produced based on the mass concentration  
226 (mascon) approach. The model provides surface mass densities on a monthly basis. Each monthly  
227 solution represents the average of surface mass densities within the month, referenced at the middle  
228 of the corresponding month. The model has been developed directly from GRACE level-1b K-Band  
229 Ranging (KBR) data. It is computed and delivered as surface mass densities per patch over blocks of  
230 approximately 1°×1° or about 12'000 km<sup>2</sup>. Although the mascon size is smaller than the inherent  
231 spatial resolution of GRACE, the model exhibits a relatively high spatial resolution. [This is attributed](#)  
232 [to a statistically optimal Wiener filtering, which uses signal and noise full covariance matrices. This](#)  
233 [allows the filter to fine tune the smoothing in line with the signal-to-noise ratio in different areas.](#)  
234 [That is, the less smoothing, the higher signal-to-noise ratio in a particular area and vice versa. This](#)  
235 [ensures that the filtering is minimal and aggressive smoothing is avoided when unnecessary. Further](#)  
236 [details of such a filter can be found in Klees et. al \(2008\). Importantly, the coloured \(frequency-](#)  
237 [dependent\) noise characteristic of KBR data was taken in to account when compiling the GRACE](#)  
238 [model, which has allowed for a reliable computation of the aforementioned noise full covariance](#)  
239 [matrices](#)~~This is attributed to a statistically optimal Wiener filtering, which uses signal and noise~~  
240 ~~covariance matrices.~~ The coloured (frequency-dependent) noise characteristic of KBR data was taken  
241 in to account when compiling the model, which has allowed for a reliable computation of these noise  
242 and signal covariance matrices. They play a crucial role when filtering and allow to achieve a higher  
243 spatial resolution compared to commonly applied GRACE filtering methods such as Gaussian  
244 smoothing and/or destriping filters. GRACE data are available for the period 01 January 2003 to 15  
245 July 2016.

### 246 3.3 Model Outputs

247 To establish the quality of the STREAM v1.3 model in runoff simulation, monthly runoff ( $R$ ) data  
248 obtained from the Global Runoff Reconstruction (GRUN\_v1, [https://doi.org/10.3929/ethz-b-](https://doi.org/10.3929/ethz-b-000324386)  
249 [000324386](https://doi.org/10.3929/ethz-b-000324386)) have been used for comparison. The GRUN dataset (Ghiggi et al., 2019) is a global  
250 monthly  $R$  dataset derived through the use of a machine learning algorithm trained with in situ  $Q$   
251 observations of relatively small catchments ( $<2500 \text{ km}^2$ ) and gridded precipitation and temperature  
252 derived from the Global Soil Wetness Project Phase 3 (GSWP3) dataset (Kim et al., 2017). The  
253 dataset covers the period from 1902 to 2014 and it is provided on a  $0.5^\circ \times 0.5^\circ$  regular grid.

## 254 4. METHOD

### 255 4.1 STREAM Model: the Concept

256 The concept behind the STREAM v1.3 model is that river discharge is a combination of hydrological  
257 responses operating at diverse time scales (Blöschl et al., 2013; Rakovec et al., 2016). In particular,  
258 river discharge can be considered made up of a *slow-flow component*, produced as outflow of the  
259 groundwater storage and of a *quick-flow component*, i.e. mainly related to the surface and subsurface  
260 runoff components (Hu and Li, 2018).

261 While the high spatial and temporal (i.e., intermittence) variability of precipitation and the highly  
262 changing land cover spatial distribution significantly impact the variability of the *quick-flow*  
263 *component* (with scales ranging from hours to days and meters to kilometres depending on the basin  
264 size), *slow-flow river discharge* reacts to precipitation inputs more slowly (i.e., months) as water  
265 infiltrates, is stored, mixed and is eventually released in times spanning from weeks to months.  
266 Therefore, the two components can be estimated by relying upon two different approaches that  
267 involve different types of observations. Based on that, within the STREAM v1.3 model, satellite soil  
268 moisture, precipitation and TWSA will be used for deriving river discharge and runoff estimates. The  
269 first two variables are used as proxy of the *quick-flow* river discharge component while TWSA is

exploited for obtaining its complementary part, i.e., the *slow-flow river discharge* component. Firstly, we exploit the role of the soil moisture in determining the response of the catchment to the precipitation inputs, which have been soundly demonstrated in more than ten years of literature studies (see e.g., [Brocca et al., 2017](#) for a comprehensive discussion on the topic). Secondly, we consider the important role of terrestrial water storage in determining the slow-flow river discharge component as modelled in several hydrological models (e.g., [Sneeuw et al., 2014](#)).

It is worth noting that this *modus operandi*, i.e. to model the *quick-flow* and *slow-flow* discharge component separately exploring their process controls independently, has been largely applied and tested in recent and past studies, e.g., for the estimation of the flow duration curve (see e.g., [Botter et al., 2007a, b](#); [Yokoo and Sivapalan 2011](#); [Muneepeerakul et al., 2010](#); [Ghotbi et al., 2020](#)).

#### 4.2 STREAM Model: the Laws

The STREAM v1.3 model is a conceptual hydrological model that, by using as input observation of  $P$ , soil moisture, TWSA and  $T_{\text{air}}$  data, simulates continuous  $R$  and  $Q$  time series.

The model entails three main components (Figure 1): 1) a snow module to separate precipitation into snowfall and rainfall, 2) a soil module to simulate the evolution in time  $t$  of the quick and slow runoff responses,  $Q_{fu}$  [mm] and  $Q_{sl}$  [mm], and 3) a routing module that transfers these components through the basins and the rivers for the simulation of the *quick-flow* river discharge,  $QF$  [ $\text{m}^3/\text{s}$ ], and the *slow-flow* river discharge,  $SF$  [ $\text{m}^3/\text{s}$ ] components.

The soil module is composed of two storages,  $S_u$  and  $S_l$  as illustrated in Figure 1. The upper storage receives inputs from  $P$ , released through a snow module ([Cislaghi et al., 2020](#)) as rainfall ( $r$ ) or stored as snow water equivalent ( $SWE$ ) within the snowpack and on the glaciers. In particular, according to [Cislaghi et al. \(2020\)](#),  $SWE$  is modelled by using as input  $T_{\text{air}}$  and a degree-day coefficient,  $C_m$ , to be estimated by calibration.

Once separated,  $r$  input contributes to the quick runoff response while the  $SWE$  (like other fluxes contributing to modify the soil water content into  $S_u$ ) is neglected as already considered in the satellite

TWSA. Therefore, the first key point of the STREAM v1.3 model is that the water content in the upper storage is directly provided by the satellite soil moisture observations and the loss processes like infiltration or evaporation do not need to be explicitly modelled to simulate the evolution in time  $t$  of soil moisture. Consequently, the quick runoff response,  $Qfu$  from the first storage can be computed following the formulation proposed by Georgakakos and Baumer (1996), as in equation (1):

$$Qfu(t) = r(t) SWI(t, T)^\alpha \quad (1)$$

where:

-  $SWI$  is the Soil Water Index (Wagner et al., 1999), i.e., the root-zone soil moisture product referred to the first layer of the model (representative of the first 5-30 centimeters of soil), derived by the surface satellite soil moisture product,  $\theta$ , by applying the exponential filtering approach in its recursive formulation (Albergel et al., 2009):

$$SWI_n = SWI_{n-1} + K_n(\theta(t_n) - SWI_{n-1}) \quad (2)$$

with the gain  $K_n$  at the time  $t_n$  given by:

$$K_n = \frac{K_{n-1}}{K_{n-1} + e^{\left(\frac{t_n - t_{n-1}}{T}\right)}} \quad (3)$$

-  $T$  [days] is a parameter, named characteristic time length, that characterizes the temporal variation of soil moisture within the root-zone profile and the gain  $K_n$  ranges between 0 and 1;

-  $\alpha[-]$  is a coefficient linked to the non-linearity of the infiltration process and it takes into account the characteristics of the soil;

- for the initialization of the filter  $K_1 = 1$  and  $SWI_1 = \theta(t_1)$ .

The second key point of STREAM v1.3 model concerns the estimation of the slow runoff response,  $Qsl$ , from the second storage. The hypothesis here, shared also with other studies (e.g., Rakovec et al., 2016), is that the dynamic of the slow runoff component can be represented by the monthly TWSA

318 data. Indeed, the time scale of slow runoff response is typically in the range of seasons to years and it  
319 can be assumed almost independent upon the water that is contained in that upper storage. For that, the  
320 slow runoff response  $Q_{sl}$ , from the second storage, can be computed following the formulation  
321 proposed by Famiglietti and Wood (1994), through equation (4) as follows:

$$322 \quad Q_{sl}(t) = \beta (TWSA^*(t))^m \quad (4)$$

323 where:

324 -  $TWSA^*$  [-] is the TWSA estimated by GRACE normalized by its minimum and maximum values.

325 The assumption behind this equation is that TWSA can be assumed as a proxy of the evolution in  
326 time,  $t$ , of the  $Sl$ , i.e., the storage of the lower storage.

327 -  $\beta$  [mm h<sup>-1</sup>] and  $m$  [-] are two parameters describing the nonlinearity between slow runoff  
328 component and  $TWSA^*$ .

329 Note that we made the hypothesis that soil moisture and TWSA observations are independent  
330 (whereas in the reality soil moisture can be responsible both for the generation of the quick flow part  
331 (mainly) and for the slow flow contribution) given the different temporal (and spatial) scales at which  
332 the quick and slow runoff responses act.

333 The STREAM v1.3 model runs in a semi-distributed version in which the catchment is divided into  
334  $s$  elements, each one representing either a subcatchment with outlet along the main channel or an area  
335 draining directly into the main channel. Each element is assumed homogeneous and hence constitutes  
336 a lumped system.

337 The routing module (controlled by a  $\gamma$  parameter) conveys the  $Q_{fu}$  and  $Q_{sl}$  response components at  
338 each element outlet (subcatchments and directly draining areas, [Brocca et al., 2011](#)) and successively  
339 at the catchment outlet of the basin. Specifically, the quick component  $Q_{fu}$  is routed to the element  
340 outlet by the Geomorphological Instantaneous Unit Hydro-graph (GIUH, [Gupta et al., 1980](#)) for  
341 subcatchments or through a linear reservoir approach ([Nash, 1957](#)) for directly draining areas; the

342  $Q_{sl}$  slow component is transferred to the outlet section by a linear reservoir approach. Finally, a  
 343 diffusive linear approach (controlled by the parameters  $C$  and  $D$ , i.e., Celerity and Diffusivity,  
 344 Troutman and Karlinger, 1985) is applied to route the quick and slow runoff components at the outlet  
 345 section of the catchment (Brocca et al., 2011). In the first case we obtain the *quick-flow* river discharge  
 346 component,  $QF$  [ $m^3/s$ ], and in the second case the *slow-flow* river discharge component,  $SF$  [ $m^3/s$ ]  
 347 (see Figure 1).

### 348 4.3 STREAM Parameters

349 The STREAM v1.3 model uses 8 parameters of which 5 are used in the soil module ( $\alpha$ ,  $T$  [days],  $\beta$   
 350 [ $mm\ h^{-1}$ ],  $m$ ,  $C_m$ ) and 3 in the routing module ( $\gamma$ ,  $C$  [ $km\ h^{-1}$ ] and  $D$  [ $km^2\ h^{-1}$ ]). The parameter values,  
 351 determined within the feasible parameter space (See Table Appendix A for more details), are  
 352 calibrated by maximizing the Kling-Gupta Efficiency index (KGE, Gupta et al., 2009; Kling et al.,  
 353 2012, see paragraph 5.1 for more details) between observed and simulated river discharge.

## 354 5. EXPERIMENTAL DESIGN

### 355 5.1 Modelling Setup for Mississippi River Basin

356 The modelling setup is carried out in four steps (Figure 2):  
 357 1. *Input data collection*. Two different groups of data have to be collected to setup the model, i.e.,  
 358 topographic information and hydrological variables. Concerning the topographic information, the  
 359 SHuttle Elevation Derivatives at multiple Scales (HydroSHED, <https://www.hydrosheds.org/>) DEM  
 360 of the basin at the 3'' resolution (nearly 90 m at the equator) as well as the location of the gauging  
 361 stations where the model should be calibrated/validated, are collected. Concerning the hydrological  
 362 variables, gridded precipitation,  $T_{air}$ , soil moisture and TWSA are collected. In addition, in situ  $Q$   
 363 time series for the sections where the model should be calibrated/validated as well as modelled runoff  
 364 datasets are required.

365 2. *Sub-basin delineation*. STREAM v1.3 model is run in the semi-distributed version over the  
366 Mississippi River basin. The TopoToolbox (<https://topotoolbox.wordpress.com/>), a tool developed in  
367 Matlab by [Schwanghart et al. \(2010\)](#), and the DEM of the basin have been used to derive flow  
368 directions, to extract the stream network and to delineate the drainage basins over the Mississippi  
369 River basin. In particular, by considering only rivers with order greater than 3 (according to the  
370 Horton-Strahler rules, [Horton, 1945](#); [Strahler, 1952](#)), the Mississippi watershed has been divided into  
371 53 sub-basins as illustrated in Figure 3. Red dots in the figure indicate the location of the 11 discharge  
372 gauging stations selected for the study area.

373 It has to be specified that the step of sub-basin delineation could be accomplished through tools  
374 different from the TopoToolbox. For instance, it could be used the free Qgis software downloadable  
375 at <https://www.qgis.org/it/site/forusers/download.html>, following the instruction to perform the  
376 hydrological analysis as in  
377 [https://docs.qgis.org/3.16/en/docs/training\\_manual/processing/hydro.html?highlight=hydrological%](https://docs.qgis.org/3.16/en/docs/training_manual/processing/hydro.html?highlight=hydrological%20analysis)  
378 [20analysis](#).

379 3. *Extraction of input data*. Precipitation,  $T_{air}$ , soil moisture and TWSA datasets data have to be  
380 extracted for each sub-basin of the study area. If characterized by different spatial/temporal  
381 resolution, these datasets need to be resampled over a common spatial grid/temporal time step prior  
382 to be used as input into the model.

383 To run the STREAM v1.3 model over the Mississippi river basin, input data have been resampled  
384 over the precipitation spatial grid at  $0.25^\circ$  resolution through a bilinear interpolation. Concerning the  
385 temporal scale,  $T_{air}$ , soil moisture and precipitation data are available at daily time step, while monthly  
386 TWSA data have been linearly interpolated at daily time step. For each of the 53 Mississippi  
387 subbasins, the resampled precipitation, soil moisture,  $T_{air}$  and TWSA data have been extracted.

388 4. *STREAM model calibration*. In situ river discharge data are used as reference data for the  
389 calibration of STREAM v1.3 model. For Mississippi, the STREAM v1.3 model has been calibrated  
390 over five sections as illustrated in Figure 3: the inner sections 4, 6, 9, 11 and the outlet section 10, are



used to calibrate the model and all sub-basins contributing to the respective sections are highlighted with the same colour. This means that, for example, the sub-basins labelled as 1, 2, 5 to 15, 17, 22, 23, and 30 contribute to section 4, sub-basins 31, 37, 38 and 41 contribute to section 6 and so on. Consequently, the sub-basins highlighted with the same colour are assigned the same model parameters, i.e. the parameters that allow to reproduce the river discharge data observed at the related outlet section.

Once calibrated, the STREAM v1.3 model has been run to provide continuous daily Q and R time series, at the outlet section of each subbasin and over each grid pixel, respectively. By considering the spatial/temporal availability of both in situ and satellite observations, the entire analysis period covers the maximum common observation period, i.e., from 01 January 2003 to 15 July 2016 at daily time scale. To establish the goodness-of-fit of the model, the simulated river discharge and runoff timeseries are compared against in situ river discharge and modelled runoff data.

## 5.2 Model Evaluation Criteria and Performance Metrics

The model has been run over a 13.5-year period split into two sub periods: the first 8 years, from January 2003 to December 2010, have been used to calibrate the model successively validated over the remaining 5.5 years (January 2011 - July 2016).

In particular, three different validation schemes have been adopted to assess the robustness of the STREAM v1.3 model:

1. Internal validation aimed to test the plausibility of both the model structure and the parameter set in providing reliable estimates of the hydrological variables against which the model is calibrated. For this purpose, a comparison between observed and simulated river discharge time series on the sections used for model calibration has been carried out for both the calibration and validation sub periods.
2. Cross-validation testing the goodness of the model structure and the calibrated model parameters to predict hydrological variables at locations not considered in the calibration phase. In this respect, the cross-validation has been carried out by comparing observed and

simulated river discharge time series in gauged basins not considered during the calibration phase;

3. External validation aimed to test the capability of the model “*to get the right answers for the right reasons*” (Kirchner 2006). In this respect, the capability of the model to reproduce variables (e.g., fluxes or state variables) other than discharge and not considered in the calibration phase, should be tested. As runoff is a secondary product of the STREAM v1.3 model, obtained indirectly from the calibration of the river discharge (basin-integrated runoff), the comparison in terms of runoff can be considered as a further external validation of the model. Runoff, differently from discharge, cannot be directly measured. It is generally modelled through land surface or hydrological models. Its validation requires a comparison against modelled data that, however, suffer from uncertainties (Beck et al., 2017). Based on that, in this study the GRUN runoff dataset described in the section 3.3 has been used for a qualitative comparison.

### 5.3 Performance Metrics

To measure the goodness-of-fit between simulated and observed river discharge data three performance scores have been used:

- the relative root mean square error, RRMSE:

$$RRMSE = \frac{\sqrt{\frac{1}{n} \sum_{i=1}^n (Q_{sim_i} - Q_{obs_i})^2}}{\frac{1}{n} \sum_{i=1}^n (Q_{obs_i})} \quad (5)$$

where  $Q_{obs}$  and  $Q_{sim}$  are the observed and simulated discharge time series of length  $n$ . RRMSE values range from 0 to  $+\infty$ , the lower the RRMSE, the better the agreement between observed and simulated data.

- the Pearson correlation coefficient,  $R$ , measures the linear relationship between two variables:

$$R = \frac{\sum_{i=1}^n (Q_{sim_i} - \overline{Q_{sim_i}})(Q_{obs_i} - \overline{Q_{obs_i}})}{\sqrt{\sum_{i=1}^n (Q_{sim_i} - \overline{Q_{sim_i}})^2 (Q_{obs_i} - \overline{Q_{obs_i}})^2}} \quad (6)$$

440 where  $\overline{Q_{obs}}$  and  $\overline{Q_{sim}}$  represent the mean values of  $Q_{obs}$  and  $Q_{sim}$ , respectively. The values of R range  
441 between  $-1$  and  $1$ ; higher values of R indicate a better agreement between observed and simulated  
442 data.

443 • the Kling-Gupta efficiency index (KGE, [Gupta et al., 2009](#)), which provides direct assessment  
444 of four aspects of discharge time series, namely shape, timing, water balance and variability. It  
445 is defined as follows:

$$446 \quad KGE = 1 - \sqrt{(R - 1)^2 + (\delta - 1)^2 + (\varepsilon - 1)^2} \quad (7)$$

447 where R is the correlation coefficient,  $\delta$  the relative variability and  $\varepsilon$  the bias normalized by the  
448 standard deviation between observed and simulated discharge. The KGE values range between  $-\infty$   
449 and  $1$ ; the higher the KGE, the better the agreement between observed and simulated data.  
450 Simulations characterized by values of KGE in the range  $-0.41$  and  $1$  can be assumed as reliable;  
451 values of KGE greater than  $0.5$  have been assumed good with respect to their ability to reproduce  
452 observed time series ([Thiemig et al., 2013](#)).

## 453 6. RESULTS

454 The testing and validation of the STREAM v1.3 model is presented and discussed in this section  
455 according to the scheme illustrated in section 5.2.

### 456 6.1 Internal Validation

457 The performance of the STREAM v1.3 model over the calibrated river sections is illustrated in Figure  
458 4 and summarized in Table 2. Figure 4 shows observed and simulated river discharge time series over  
459 the whole study period (2003-2016); in Table 2 the performance scores are evaluated separately for  
460 the calibration and validation sub periods. It is worth noting that the model accurately simulates the  
461 observed river discharge data and is able to give the “right answer” with good modelling  
462 performances. Score values of KGE and R over the calibration (validation) period are higher than  
463  $0.62$  ( $0.67$ ) and  $0.75$  ( $0.75$ ) (resp.) for all the sections; RRMSE is lower than  $46\%$  ( $51\%$ ) for all the  
464 sections except for section 9, where it rises up to  $71\%$  ( $77\%$ ). The performances remain good even if

they are evaluated over the entire study period as indicated by the scores on the top of each plot of Figure 4.

## 6.2 Cross-validation

The cross-validation has been carried out over the six river sections illustrated in Figure 5 not used in the calibration step. The performance scores on the top of each plot refer to the entire study periods; the scores split for calibration and validation periods are reported in Table 2. For some river sections the performance is quite low (see, e.g., river section 1, 2 and 5) whereas for others the model is able to simulate the observed discharge data quite accurately (e.g., 7 and 8). In particular, for river sections 1 and 2 even if KGE reaches values equal to 0.35 and 0.40 (for the whole period), respectively, there is not a good agreement between observed and simulated river discharge and the R score is lower than 0.55 for both river sections. The worst performance is obtained over section 5, with negative KGE and low R (high RRSME). These results are certainly influenced by the presence of large dams located upstream to these river sections (i.e., Garrison, Gavins Point and Kanopolis dams, see Table 1) which have a strong impact on discharge: the model, not having a specific module for modelling reservoirs, is not able to accurately reproduce the dynamics of river discharge over regulated river sections. Positive KGE values are obtained over river sections 3, 7 and 8. In particular, over sections 3 (influenced by the presence of dams in section 1 and 2) the STREAM v1.3 model overestimates the observed river discharge due the presence of large dams along the Missouri river. Over section and 7 (located over the Rock river, a relatively small tributary of Mississippi river (see Table 1), the STREAM v1.3 model overestimates overestimation has to be attributed to: 1) the different characteristics of the Rock river basin with respect to the entire basin closed to section 6 where the model has been calibrated (see Figure 3); 2) the small size of the Rock river basin (23'000 km<sup>2</sup>, if compared with GRACE resolution, 160'000 km<sup>2</sup>) for which the model accuracy is expect to be lower. the observed river discharge highlighting that the model parameters estimated for river section 4 and 6, respectively, are not suitable to accurately reproduce river discharge for river sections 3 and 7 (see Figure 3 and Figure 5). Conversely, the performances over river section 8, whose

parameters have been set equal to the ones of river section 10, are quite high (KGE equal to 0.71, 0.80 and 0.77 for the entire, the calibration and the validation period, respectively; R equal to 0.83, 0.84 and 0.84 for the entire, calibration and validation periods, respectively).

Although it is expected that the performances of STREAM v1.3 model, as any hydrological model calibrated against observed data, can decrease over the gauging sections not used for the calibration, the findings obtained above raises doubts about the robustness of model parameters and whether it is actually possible to transfer model parameters from one river section to another with different interbasin characteristics. [A more in-depth investigation about the model calibration procedure, with special focus on the regionalization of the model parameters, should be carried out but this topic is beyond the scope of the manuscript](#)~~A more in-depth investigation about the model calibration procedure and the regionalization of the model parameters will be carried out in future studies.~~

### 6.3 External Validation

For the external validation, the monthly runoff time series provided by the GRUN datasets have been compared against the ones computed by the STREAM v1.3 model. For that, STREAM daily runoff time series have been aggregated at monthly scale and re-gridded at the same spatial resolution of the GRUN dataset (0.5°). The comparison is illustrated in Figure 6 for the common period 2003–2014. Although the two datasets consider different precipitation inputs, the two models agree in identifying two distinct zones in terms of runoff, i.e., the western dry and the eastern wet area. This two distinct zones can be clearly identified also in the GSWP3 and TMPA 3B42 V7 precipitation maps (not shown here) used as input in GRUN and STREAM v1.3, respectively, stressing that STREAM runoff output is correctly driven by the input data. However, likely due to the calibration procedure, the STREAM runoff map appears patchier with respect to GRUN and discontinuities along the sub-basin boundaries (identified in Figure 3) can be noted. This should be ascribed to the automatic calibration procedure of the model that, differently from other calibration techniques (e. g., regionalization procedures), does not consider the basin physical attributes like soil, vegetation, and geological properties that govern spatial dynamics of hydrological processes. This calibration procedure can generate sharp

discontinuities even for neighbouring subcatchments individually calibrated. It leads to discontinuities in model parameter values and consequently in the simulated hydrological variable (runoff).

## 7. DISCUSSION

In the previous sections, the ability of the STREAM v1.3 model to accurately simulate river discharge and runoff time series has been presented. In particular, Figures 4, 5 and 6 demonstrate that satellite observations of precipitation, soil moisture and terrestrial water storage anomalies can provide accurate daily river discharge estimates for near-natural large basins (absence of upstream dams), and for basins with draining area lower than 160'000 km<sup>2</sup> (see section 7), i.e., at spatial/temporal resolution lower than the ones of the TWSA input data (monthly, 160'000 km<sup>2</sup>). This is an important result of the study as it demonstrates, on one hand, that the model structure is appropriate with respect to the data used as input and, on the other hand, the great value of information contained into TWSA data that, even if characterized by limited spatial/temporal resolution, can be used to simulate runoff and river discharge at basin scale. This finding has been also confirmed by a preliminary sensitivity analysis in which the STREAM v1.3 model has been run with different hydrological inputs of precipitation, soil moisture and total water storage anomaly (not shown here for brevity). In particular, by running the STREAM v1.3 model with different input configurations (e.g., by using TMPA 3B42 V7 or Climate Prediction Center (CPC) data for precipitation, ESA CCI or Advanced SCATterometer (ASCAT) data for soil moisture, TWSA or soil moisture data to simulate the slow-flow river discharge component), we found that STREAM results are more sensitive to soil moisture data rather than to precipitation input. In addition, by running STREAM v1.3 model with soil moisture data as input to simulate the slow-flow river discharge component (i.e. without using TWSA data) we found a deterioration of the model results.

Hereinafter, the strengths and the main limitations of the STREAM v1.3 model are discussed.

Among the strengths of the STREAM v1.3 model it is worth highlighting:

542 1. **Remote sensing-based conceptual hydrological model.** Discharge and runoff estimates are  
543 obtained through a remote sensing-based conceptual hydrological model, simpler than classical  
544 hydrological models or LSMs. In particular, discharge and runoff estimates are obtained by exploiting  
545 as much as possible satellite observations and by keeping the modelling component at a minimum.  
546 The knowledge of the key mechanisms and processes that act in the formation of runoff, like the role  
547 of the soil moisture in determining the response of the catchment to precipitation, played a major role  
548 in the definition of the model structure. Being an observational-based approach, the STREAM v1.3  
549 model presents two main advantages: 1) possibility to directly ingest observations (soil moisture and  
550 terrestrial water storage data) into the model structure, allowing to take implicitly into account some  
551 processes, mainly human-driven (e.g., irrigation, change in the land use), which might have a large  
552 impact on the hydrological cycle and hence on total runoff; 2) the independence with respect to  
553 existing large scale hydrological models such as, e.g., the evapotranspiration is not explicitly  
554 modelled.

555 2. **Simplicity.** The STREAM v1.3 model structure: 1) limits the input data required (only  
556 precipitation,  $T_{\text{air}}$ , soil moisture and TWSA data are needed as input; LSM/GHMs require many  
557 additional inputs such as wind speed, shortwave and longwave radiation, pressure and relative  
558 humidity); 2) limits and simplifies the processes to be modelled for runoff/discharge simulation.  
559 Processes like evapotranspiration, infiltration or percolation, are not modelled therefore avoiding the  
560 need of using sophisticated and highly parameterized equations (e.g., Penman-Monteith for  
561 evapotranspiration, [Allen et al., 1998](#), Richard equation for infiltration, [Richard, 1931](#)); 3) limits the  
562 number of parameters (only 8 parameters have to be calibrated) thus simplifying the calibration  
563 procedure and potentially reduce the model uncertainties related to the estimation of parameter  
564 values.

565 3. **Versatility.** The STREAM v1.3 model is a versatile model suitable for daily runoff and discharge  
566 estimation over sub-basins with different physiographic characteristics. The results obtained in this

study clearly indicate the potential of this approach to be extended at the global scale. Moreover, the model can be easily adapted to ingest input data with spatial/temporal resolution different from the one tested in this study (0.25°/daily). For instance, satellite missions with higher space/time resolution, or near real time satellite products could be considered. As an example, the Next Generation Gravity Mission design studies all encompass double-pair scenarios, which would greatly improve upon the current spatial resolution of single-pair missions like GRACE and GRACE-FO (> 100'000 km<sup>2</sup>).

**4. Computationally inexpensive.** Due to its simplicity and the limited number of parameters to be calibrated, the computational effort for the STREAM v1.3 model is very limited.

However, some limitations have to be acknowledged for the current version of the STREAM v1.3 model:

**1. Presence of reservoir, diversion, dams or flood plain.** As the STREAM v1.3 model does not explicitly consider the presence of discontinuity elements along the river network (e. g, reservoir, dam or floodplain), discharge estimates obtained for sections located downstream of such elements might be inaccurate (see, e.g., river sections 1 and 2 in Figure 5).

**2. Need of in situ data for model calibration and robustness of model parameters.** As discussed in the results section, parameter values of the STREAM v1.3 model are set through an automatic calibration procedure aimed at minimizing the differences between simulated and observed river discharge. The main drawback of this parameterization technique is that the models parameterized with this technique may exhibit (1) poor predictability of state variables and fluxes at locations and periods not considered in the calibration, and (2) sharp discontinuities along sub-basin boundaries in state flux, and parameter fields (e.g., [Merz and Blöschl, 2004](#)).

To overcome these issues, several regionalization procedures, as for instance summarized in [Cislaghi et al. \(2020\)](#), could be conveniently applied to transfer model parameters from hydrologically similar catchments to a catchment of interest. In particular, the regionalization of model parameters could



allow to: i) estimate discharge and runoff time series over ungauged basins overcoming the need of discharge data recorded from in-situ networks; ii) estimate the model parameter values through a physically consistent approach, linking them to the characteristics of the basins; iii) solve the problem of discontinuities in the model parameters, avoiding to obtain patchy unrealistic runoff maps. [As this aspect requires additional investigations and it is beyond the paper purpose, it will not be tackled here](#)~~However, this aspect is beyond the paper purpose and it will conveniently addressed in future works.~~

## 8. CONCLUSIONS

This study presents a new conceptual hydrological model, STREAM v1.3, for runoff and river discharge estimation. By using as input satellite data of precipitation, soil moisture and terrestrial water storage anomalies, the model has been able to provide accurate daily river discharge and runoff estimates at the outlet river section and the inner river sections and over a  $0.25^{\circ} \times 0.25^{\circ}$  spatial grid of the Mississippi river basin. In particular, the model is suitable to reproduce:

1. river discharge time series over the calibrated river section with good performances both in calibration and validation periods;
2. river discharge time series over river sections not used for calibration and not located downstream dams or reservoirs;
3. runoff time series with a quite good agreement with respect to the well-established GRUN observational-based dataset used for comparison.

The integration of observations of soil moisture, precipitation and terrestrial water storage anomalies is a first alternative method for river discharge and runoff estimation with respect to classical methods based on the use of TWSA-only (suitable for river basins larger than 160'000 km<sup>2</sup>, monthly time scale) or on classical LSMs (Cai et al., 2014).

Moreover, although simple, the model has demonstrated a great potential to be easily applied over subbasins with different climatic and topographic characteristics, suggesting also the possibility to

618 extend its application to other basins. In particular, the analysis over basins with high human impact,  
619 where the knowledge of the hydrological cycle and the river discharge monitoring is very important,  
620 deserves special attention. Indeed, as the STREAM v1.3 model is directly ingesting observations of  
621 soil moisture and terrestrial water storage data, it allows the modeller to neglect processes that are  
622 implicitly accounted for in the input data. Therefore, human-driven processes (e.g., irrigation, land  
623 use change), that are typically very difficult to simulate due to missing information and might have a  
624 large impact on the hydrological cycle, hence on total runoff, could be implicitly modelled. The  
625 application of the STREAM v1.3 model on a larger number of basins with different climatic-  
626 physiographic characteristics (e.g., including more arid basins, snow-dominated, lots of topography,  
627 heavily managed) will allow to investigate the possibility to regionalize the model parameters and  
628 overcome the limitations of the automatic calibration procedure highlighted in the discussion  
629 section~~will be object of future studies and it will allow to investigate the possibility to regionalize the~~  
630 ~~model parameters and overcome the limitations of the automatic calibration procedure highlighted in~~  
631 ~~the discussion section.~~

## 632 AUTHOR CONTRIBUTION

633 S.C. performed the analysis and wrote the manuscript. G.G. collected the data and helped in  
634 performing the analysis; C.M, L.B., A.T., N.S., H.H.F., C.M., M.R. and J.B. contributed to the  
635 supervision of the work. All authors discussed the results and contributed to the final manuscript.

## 636 CODE AVAILABILITY

637 The STREAM model version 1.3, with a short user manual, is freely downloadable in Zenodo  
638 (<https://zenodo.org/record/4744984>, doi: 10.5281/zenodo.4744984). The STREAM v1.3 model code  
639 is distributed through M language files, but it could be run with different interpreters of M language,  
640 like the GNU Octave (freely downloadable here <https://www.gnu.org/software/octave/download>).

641 **DATA AVAILABILITY**

642 All data and codes used in the study are freely available online. Air temperature data are available at  
643 <https://psl.noaa.gov/data/gridded/data.cpc.globaltemp.html> (last access 25/11/202). In situ river  
644 discharge data have been taken from the Global Runoff Data Center (GRDC,  
645 [https://www.bafg.de/GRDC/EN/Home/homepage\\_node.html](https://www.bafg.de/GRDC/EN/Home/homepage_node.html) (last access 25/11/202). Precipitation  
646 and soil moisture data are available from <http://pmm.nasa.gov/data-access/downloads/trmm> and  
647 <https://esa-soilmoisture-cci.org/>, respectively.

648 **COMPETING INTERESTS**

649 The authors declare that they have no conflict of interest.

650 **ACKNOWLEDGMENTS**

651 The authors wish to thank the Global Runoff Data Centre (GRDC) for providing most of the  
652 streamflow data throughout Europe. The authors gratefully acknowledge support from ESA through  
653 the STREAM Project (EO Science for Society element Permanent Open Call contract n°  
654 4000126745/19/I-NB).

655

656 REFERENCE

657 ~~Botter, G., Porporato, A., Daly, E., Rodriguez-Iturbe, I., and Rinaldo, A. (2007a). Probabilistic characterization of base~~  
658 ~~flows in river basins: Roles of soil, vegetation, and geomorphology, Water Resour. Res., 43,~~  
659 ~~W06404,doi:10.1029/2006WR005397.~~

660 Albergel, C., Rüdiger, C., Carrer, D., Calvet, J. C., Fritz, N., Naeimi, V., Bartalis, Z., and Hasenauer, S. (2009).: An  
661 evaluation of ASCAT surface soil moisture products with in-situ observations in southwestern France. , Hydrol. Earth  
662 Syst. Sci.Hydrology and Earth System Sciences, 13, 115–124, <https://doi.org/doi:10.5194/hess-13-115-2009>, 2009..

663 Alexander, J. S., Wilson, R. C., and Green, W. R.: A brief history and summary of the effects of river engineering and  
664 dams on the Mississippi River system and delta (p. 53), US Department of the Interior, US Geological Survey,  
665 <https://doi.org/10.3133/cir1375>, 2012.

666 Allen, R.G., Pereira, L. S., Raes, D., and Smith, M: Crop evapotranspiration — guidelines for computing crop water  
667 requirements. FAO Irrigation & Drainage Paper 56. FAO, Rome, 1988.

668 Balsamo, G., A. Beljaars, K. Scipal, P. Viterbo, B. vanden Hurk, M. Hirschi, and A. K. Betts: A revised hydrology for  
669 the ECMWF model: Verification from field site to terrestrial water storage and impact in the integrated forecast  
670 system, J. Hydrometeorol., 10(3), 623–643, <https://doi.org/doi:10.1175/2008JHM1068.1>, 2009.

671 Barbarossa, V., Huijbregts, M. A., Beusen, A. H., Beck, H. E., King, H., and Schipper, A. M.: FLO1K, global maps of  
672 mean, maximum and minimum annual streamflow at 1 km resolution from 1960 through 2015, Scientific Sci. Data,  
673 55, 180052, <https://doi.org/10.1038/sdata.2018.52>, 2018.

674 Beck, H. E., van Dijk, A. I., de Roo, A., Dutra, E., Fink, G., Orth, R., and Schellekens, J.: Global evaluation of runoff  
675 from ten state-of-the-art hydrological models, Hydrol. Earth Syst. Sci., 21(6), 2881-2903. [https://doi.orgdoi:](https://doi.orgdoi:doi.org/10.5194/hess-21-2881-2017)  
676 [doi.org/10.5194/hess-21-2881-2017](https://doi.org/10.5194/hess-21-2881-2017), 2017.

677 Berghuijs, W. R., Woods, R. A., Hutton, C. J., and Sivapalan, M.: Dominant flood generating mechanisms across the  
678 United States, Geophys. Res. Lett., 43, 4382–4390, <https://doi.org/10.1002/2016GL068070>, 2016.

679 Berthet, L., Andréassian, V., Perrin, C., and Javelle, P.: How crucial is it to account for the antecedent moisture conditions  
680 in flood forecasting? Comparison of event-based and continuous approaches on 178 catchments, Hydrol. Earth Syst.  
681 Sci., 13(6), 819-831, 2009.

682 Blöschl, G., Sivapalan, M., Wagener, T., Viglione, A., and Savenije, H. H. G. (Eds.): Runoff predictions in ungauged  
683 basins: A synthesis across processes, places and scales, Cambridge: Cambridge University Press, 2013.

684 Botter, G., Porporato, A., Daly, E., Rodriguez-Iturbe, I., and Rinaldo, A.: Probabilistic characterization of base flows in  
685 river basins: Roles of soil, vegetation, and geomorphology, Water Resour. Res., 43, W06404,  
686 <https://doi.org/doi:10.1029/2006WR005397>, 2007a.

687 Botter, G., Peratoner, F., Porporato, A., Rodriguez-Iturbe, I., and Rinaldo, A.: Signatures of large-scale soil moisture  
688 dynamics on streamflow statistics across U.S. Climate regimes, Water Resour. Res., 43, W11413,  
689 <https://doi.org/doi:10.1029/2007WR006162>, 2007b.

690 Brocca, L., Ciabatta, L., Massari, C., Camici, S., and Tarpanelli, A.: Soil moisture for hydrological applications: open  
691 questions and new opportunities, Water, 9(2), 140, <https://doi.org/10.3390/w9020140>, 2017.

692 Brocca, L., Melone, F., and Moramarco, T.: Distributed rainfall-runoff modelling for flood frequency estimation and  
693 flood forecasting, Hydrol. Process., 25(18), 2801-2813, <https://doi.org/10.1002/hyp.8042>, 2011.

694 Brocca, L., Melone, F., and Moramarco, T.: On the estimation of antecedent wetness conditions in rainfall-runoff  
695 modelling, Hydrol. Process., 22 (5), 629-642, doi:10.1002/hyp.6629. <https://doi.org/10.1002/hyp.6629>, 2008.

696 Brocca, L., Melone, F., Moramarco, T., and Morbidelli, R.: Antecedent wetness conditions based on ERS scatterometer  
697 data, J. Hydrol., 364(1-2), 73-87, <https://doi.org/10.1016/j.jhydrol.2008.10.007>, 2009.

698 Cai, X., Yang, Z. L., David, C. H., Niu, G. Y., and Rodell, M.: Hydrological evaluation of the Noah-MP land surface  
699 model for the Mississippi River Basin, J. Geophys. Res. Atmos., 119(1), 23-38,  
700 <https://doi.org/10.1002/2013JD020792>, 2014.

Formattato: Inglese (Stati Uniti)

Formattato: Inglese (Stati Uniti)

Codice campo modificato

Formattato: Inglese (Stati Uniti)

Codice campo modificato

Formattato: Inglese (Stati Uniti)

Formattato: Inglese (Stati Uniti)

- Cislaghi, A., Masseroni, D., Massari, C., Camici, S., and Brocca, L.: Combining a rainfall-runoff model and a regionalization approach for flood and water resource assessment in the western Po Valley, Italy, *Hydrol. Sci. J.*, 65(3), 348-370, <https://doi.org/10.1080/02626667.2019.1690656>, 2020.
- Crochemore, L., Isberg, K., Pimentel, R., Pineda, L., Hasan, A., and Arheimer, B.: Lessons learnt from checking the quality of openly accessible river flow data worldwide, *Hydrol. Sci. J.*, 65(5), 699-711, <https://doi.org/10.1080/02626667.2019.1659509>, 2020.
- Crow, W. T., Bindlish, R., and Jackson, T. J.: The added value of spaceborne passive microwave soil moisture retrievals for forecasting rainfall-runoff partitioning, *Geophys. Res. Lett.*, 32(18), <https://doi.org/10.1029/2005GL023543>, 2005.
- Döll, P., F.Kaspar, and B.Lehner: A global hydrological model for deriving water availability indicators: Model tuning and validation, *J. Hydrol.*, 270(1-2), 105-134, [https://doi.org/doi:10.1016/S0022-1694\(02\)00283-4](https://doi.org/doi:10.1016/S0022-1694(02)00283-4), 2003.
- Dorigo, W., Wagner, W., Albergel, C., Albrecht, F., Balsamo, G., Brocca, L., Chung, D., Ertl, M., Forkel, M., Gruber, A., Haas, D., Hamer, P., Hirschi, M., Ikonen, J., de Jeu, R., Kidd, R., Lahoz, W., Liu, Y.Y., Miralles, D., Mistelbauer, T., Nicolai-Shaw, N., Parinussa, R., Pratola, C., Reimer, C., van der Schalie, R., Seneviratne, S.I., Smolander, T., and Lecomte, P.: ESA CCI Soil Moisture for improved Earth system understanding: state-of-the art and future directions., *Remote Sens. Environ.*, 203, 185-215, <https://doi.org/10.1016/j.rse.2017.07.001>, 2017.
- Dyer, J.: Snow depth and streamflow relationships in large North American watersheds, *J. Geophys. Res.*, 113, D18113, <https://doi.org/10.1029/2008JD010031>, 2008.
- Entekhabi, D., Njoku, E. G., O'Neill, P. E., Kellogg, K. H., Crow, W. T., Edelstein, W. N., ... and Van Zyl, J.: The soil moisture active passive (SMAP) mission, *Proceedings of the Institute of Electrical and Electronics Engineers (IEEE)*, 98(5), 704-716, <https://doi.org/doi:10.1109/JPROC.2010.2043918>, 2010.
- Famiglietti, J. S., and Rodell, M.: Water in the balance, *Science*, 340(6138), 1300-1301, <https://doi.org/10.1126/science.1236460>, 2013.
- Famiglietti, J.S., and Wood, E. F.: Multiscale modeling of spatially variable water and energy balance processes, *Water Resour. Res.*, 30, 3061-3078, <https://doi.org/10.1029/94WR01498>, 1994.
- Fan, Y. and Van den Dool, H. A.: Global monthly land surface air temperature analysis for 1948-present, *J. Geophys. Res. Atmos.*, 113, D01103, <https://doi.org/10.1029/2007JD008470>, 2008.
- Fekete, B. M., Looser, U., Pietroniro, A., and Robarts, R. D.: Rationale for monitoring discharge on the ground, *J. Hydrometeorol.*, 13, 1977-1986, <https://doi.org/10.1175/JHM-D-11-0126.1>, 2012.
- Georgakakos KP, and Baumer OW.: Measurement and utilization of onsite soil moisture data, *J. Hydrol.*, 184: , 131-152, [https://doi.org/10.1016/0022-1694\(95\)02971-0](https://doi.org/10.1016/0022-1694(95)02971-0), 1996.
- Ghiggi, G., Humphrey, V., Seneviratne, S. I., and Gudmundsson, L.: GRUN: an observation-based global gridded runoff dataset from 1902 to 2014, *Earth Syst. Sci. Data*, 11, 1655-1674, *Earth System Science Data*, 11(4), 1655-1674, <https://doi.org/10.5194/essd-11-1655-2019>, 2019.
- Ghotbi, S., Wang, D., Singh, A., Blöschl, G., and Sivapalan, M.: A New Framework for Exploring Process Controls of Flow Duration Curves, *Water Resour. Res.*, 56(1), <https://doi.org/e2019WR026083>, 2020.
- Gudmundsson, L., Wagener, T., Tallaksen, L. M., and Engeland, K.: Evaluation of nine large-scale hydrological models with respect to the seasonal runoff climatology in Europe, *Water Resour. Res.*, 48(11), <https://doi.org/10.1029/2011WR010911>, 2012a.
- Gudmundsson, L., Tallaksen, L. M., Stahl, K., Clark, D. B., Du-mont, E., Hagemann, S., Bertrand, N., Gerten, D., Heinke, J., Hanasaki, N., Voss, F., and Koirala, S.: Comparing Large-Scale Hydrological Model Simulations to Observed Runoff Percentiles in Europe, *J. Hydrometeorol.*, 13, 604-62, <https://doi.org/10.1175/JHM-D-11-083.1>, 2012b.
- Gudmundsson, L., and Seneviratne, S. I.: Observation-based gridded runoff estimates for Europe (E-RUN version 1.1), *Earth Syst. Sci. Data*, 8, 279-295, <https://doi.org/10.5194/essd-8-279-2016>, 8(2), 279-295, 2016.
- Gupta VK, Waymire E, and Wang CT.: A representation of an instantaneous unit hydrograph from geomorphology, *Water Resour. Res.*, 16: 855-862, <https://doi.org/doi:10.1029/WR016i005p00855>, 1980.

Gupta, H. V., Kling, H., Yilmaz, K. K., and Martinez, G. F.: Decomposition of the mean squared error and NSE performance criteria: Implications for improving hydrological modelling, *J. Hydrol.*, 377(1-2), 80-91, <https://doi.org/10.1016/j.jhydrol.2009.08.003>, 2009.

Haddeland, I., Heinke, J., Voß, F., Eisner, S., Chen, C., Hagemann, S., and Ludwig, F.: Effects of climate model radiation, humidity and wind estimates on hydrological simulations, *Hydrol. Earth Syst. Sci.*, 16(2), 305-318, <https://doi.org/10.5194/hess-16-305-2012>, 2012.

Hastie, T., Tibshirani, R., and Friedman, J. H.: *The Elements of Statistical Learning – Data Mining, Inference, and Prediction*, Second Edition, Springer Series in Statistics, Springer, New York, 2nd Edn., available at: <http://www-stat.stanford.edu/~tibs/ElemStatLearn/> (last access: 5 July 2016), 2009.

Hong, Y., Adler, R. F., Hossain, F., Curtis, S., and Huffman, G. J.: A first approach to global runoff simulation using satellite rainfall estimation, *Water Resour. Res.*, 43(8), <https://doi.org/10.1029/2006WR005739>, 2007.

Horton, R. E.: Hydrological approach to quantitative morphology, *Geol. Soc. Am. Bull.*, 56, 275-370, 1945.

Houborg, R., Rodell, M., Li, B., Reichle, R., and Zaitchik, B. F.: Drought indicators based on model-assimilated Gravity Recovery and Climate Experiment (GRACE) terrestrial water storage observations, *Water Resour. Res.*, 48(7), <https://doi.org/10.1029/2011WR011291>, 2012.

Hu GR., and Li XY.: Subsurface Flow, In: Li X., Vereecken H. (eds) *Observation and Measurement. Ecohydrology*. Springer, Berlin, Heidelberg, [https://doi.org/10.1007/978-3-662-47871-4\\_9-1](https://doi.org/10.1007/978-3-662-47871-4_9-1), 2018.

Huffman, G. J., Adler, R. F., Bolvin, D. T., Gu, G. J., Nelkin, E. J., Bowman, K. P., Hong, Y., Stocker, E. F. and Wolff, D. B.: The TRMM Multisatellite Precipitation Analysis (TMPA): Quasi-Global, Multiyear, Combined-Sensor Precipitation Estimates at Fine Scales, *J. Hydrometeorol.*, 8 (1): 38–55. <https://doi.org/doi:10.1175/jhm560.1>, 2007.

Huffman, G. J., Stocker, E. F., Bolvin, D. T., Nelkin, E. J., and Adler, R. F.: TRMM Version 7 3B42 and 3B43 Data Sets, NASA/GSFC, Greenbelt, MD, 2014.

Huffman, G. J., Bolvin, D. T., Braithwaite D., Hsu K., Joyce R., Kidd C., Nelkin Eric J., Sorooshian S., Tan J., and Xie P.: NASA Global Precipitation Measurement (GPM) Integrated Multi-satellite Retrievals for GPM (IMERG)., [https://docserver.gesdisc.eosdis.nasa.gov/public/project/GPM/IMERG\\_ATBD\\_V06.pdf](https://docserver.gesdisc.eosdis.nasa.gov/public/project/GPM/IMERG_ATBD_V06.pdf), 2019.

Kim, H., Watanabe, S., Chang, E. C., Yoshimura, K., Hirabayashi, J., Famiglietti, J., and Oki, T.: Global Soil Wetness Project Phase 3 Atmospheric Boundary Conditions (Experiment 1) [Data set], Data Integration and Analysis System (DIAS), <https://doi.org/10.20783/DIAS.501>, 2017.

Kirchner, J. W.: Getting the right answers for the right reasons: Linking measurements, analyses, and models to advance the science of hydrology, *Water Resour. Res.*, 42(3), <https://doi.org/10.1029/2005WR004362>, 2006.

Klees, R., Revtova, E. A., Gunter, B. C., Ditmar, P., Oudman, E., Winsemius H. C., and Savenije H.H.G.: The design of an optimal filter for monthly GRACE gravity models, *Geoph. J. Intern.*, 175 (2): 417–432, <https://doi.org/10.1111/j.1365-246X.2008.03922.x>, 2008.

Kling, H., Fuchs, M., and Paulin, M.: Runoff conditions in the upper Danube basin under an ensemble of climate change scenarios, *J. Hydrol.*, 424, 264-277, <https://doi.org/doi:10.1016/j.jhydrol.2012.01.011>, 2012.

Landerer, F. W., and Swenson, S. C.: Accuracy of scaled GRACE terrestrial water storage estimates, *Water Resour. Res.*, 48(4), <https://doi.org/10.1029/2011WR011453>, 2012.

Lehner, B., C. Reidy Liermann, C. Revenga, C. Vörösmarty, B. Fekete, P. Crouzet, P. Döll, M. Endejan, K. Frenken, J. Magome, C. Nilsson, J.C. Robertson, R. Rodel, N. Sindorf, and D. Wisser.: High-resolution mapping of the world's reservoirs and dams for sustainable river-flow management, *Front. Ecol. Environ.*, 9 (9): 494-502, <https://doi.org/10.1890/100125>, 2011.

Long, D., Longuevergne, L., and Scanlon, B. R.: Uncertainty in evapotranspiration from land surface modeling, remote sensing, and GRACE satellites, *Water Resour. Res.*, 50(2), 1131-1151, <https://doi.org/10.1002/2013WR014581>, 2014.

Lorenz, C., H. Kunstmann, H., B. Devaraju, B., ~~M. J.~~ Tourian, ~~M. J.~~ N. Sneeuw, N., and J. Riegger, J.: Large-Scale Runoff from Landmasses: A Global Assessment of the Closure of the Hydrological and Atmospheric Water Balances., *J. Hydrometeorol.*, 15, 2111–2139, <https://doi.org/doi:10.1175/JHM-D-13-0157.1>, 2014.

**Codice campo modificato**

**Formattato:** Nessuna sottolineatura, Colore carattere: Automatico

Luthcke, S.B., Sabaka, T.J., Loomis, B.D., Arendt, A.A., McCarthy, J.J., and Camp, J.: Antarctica, Greenland and Gulf of Alaska land-ice evolution from an iterated GRACE global mascon solution, *J. Glaciol.*, Vol. 59, No. 216, 613–631, 2013 <https://doi.org/doi:10.3189/2013JoG12J147>, 2013.

Massari, C., Brocca, L., Barbetta, S., Papathanasiou, C., Mimikou, M., and Moramarco, T.: Using globally available soil moisture indicators for flood modelling in Mediterranean catchments, *Hydrol. Earth Syst. Sci.*, 18(2), 839, <https://doi.org/10.5194/hess-18-839-2014>, 2014.

Massari, C., Brocca, L., Tarpanelli, A., Hong, Y., Crow, W., Ciabatta, L., Camici, S., Barbetta, S., and Moramarco, T.: Global surface runoff estimation in near real time by using SMAP and GPM, poster at SMAP conference, 2016.

Merz, R., and Blöschl, G.: A regional analysis of event runoff coefficients with respect to climate and catchment characteristics in Austria, *Water Resour. Res.*, 45(1), <https://doi.org/10.1029/2008WR007163>, 2009.

Mueller Schmied, H., Adam, L., Eisner, S., Fink, G., Flörke, M., Kim, H., ... and Song, Q.: Variations of global and continental water balance components as impacted by climate forcing uncertainty and human water use, *Hydrol. Earth Syst. Sci.*, 20(7), 2877–2898, <https://doi.org/10.5194/hess-20-2877-2016>, 2016.

Muneepeerakul, R., Azale, S., Botter, G., Rinaldo, A., and Rodriguez-Iturbe, I.: Daily streamflow analysis based on a two-scaled gamma pulse model, *Water Resour. Res.*, 46(11), <https://doi.org/10.1029/2010WR009286>, 2010.

Nash, J. E.: The form of the instantaneous unit hydrograph, IASH publication no. 45, 3–4, 114–121, 1957.

Natural Resources Conservation Service (NRCS): Urban hydrology for small watersheds, Tech. Release 55, 2nd ed., U.S. Dep. of Agric., Washington, D. C. (available at [ftp://ftp.wcc.nrcs.usda.gov/downloads/hydrology\\_hydraulics/tr55/tr55.pdf](ftp://ftp.wcc.nrcs.usda.gov/downloads/hydrology_hydraulics/tr55/tr55.pdf)), 1986.

Orth, R., and Seneviratne, S. I.: Introduction of a simple-model-based land surface dataset for Europe, *Environ. Res. Lett.*, 10(4), 044012, <https://doi.org/10.1088/1748-9326/10/4/044012>, 2015.

Pellet, V., Aires, F., Munier, S., Fernández Prieto, D., Jordá, G., Dorigo, W. A., ... and Brocca, L.: Integrating multiple satellite observations into a coherent dataset to monitor the full water cycle—application to the Mediterranean region., *Hydrol. Earth Syst. Sci.*, 23(1), 465–491, <https://doi.org/10.5194/hess-23-465-2019>, 2019.

Prudhomme, C., Giuntoli, I., Robinson, E. L., Clark, D. B., Arnell, N. W., Dankers, R., ... and Hagemann, S.: Hydrological droughts in the 21st century, hotspots and uncertainties from a global multimodel ensemble experiment, *Proceedings of the National Academy of Sciences*, 111(9), 3262–3267, 2014.

Rakovec, O., Kumar, R., Attinger, S., and Samaniego, L.: Improving the realism of hydrologic model functioning through multivariate parameter estimation, *Water Resour. Res.*, 52(10), 7779–7792, <https://doi.org/10.1002/2016WR019430>, 2016.

Richards, L.A.: Capillary conduction of liquids through porous mediums, *Physics*, 1 (5): 318–333., Bibcode:1931Physi.1.318R., <https://doi.org/doi:10.1063/1.1745010>, 1931.

Riegger, J., and M.-J.-Tourian, M. J.: Characterization of runoff-storage relationships by satellite gravimetry and remote sensing, *Water Resour. Res.*, 50, 3444–3466, <https://doi.org/doi:10.1002/2013WR013847>, 2014.

Rodell, M., Beaudoin, H. K., L’Ecuyer, T. S., Olson, W. S., Famiglietti, J. S., Houser, P. R., Adler, R., Bosilovich, M. G., Clayson, C. A., Chambers, D., Clark, E., Fetzer, E. J., Gao, X., Gu, G., Hilburn, K., Huffman, G. J., Lettenmaier, D. P., Liu, W. T., Robertson, F. R., Schlosser, C. A., Sheffield, J. and Wood, E. F.: The observed state of the water cycle in the early 15twenty-first century, *J. Clim.*, 28(21), 8289–8318, <https://doi.org/doi:10.1175/JCLI-D-14-00555.1>, 2015.

Schellekens, J., Dutra, E., Martínez-de la Torre, A., Balsamo, G., van Dijk, A., Sperna Weiland, F., Minvielle, M., Calvet, J.-C., Decharme, B., Eisner, S., Fink, G., Flörke, M., Peßenteiner, S., van Beek, R., Polcher, J., Beck, H., Orth, R., Calton, B., Burke, S., Dorigo, W., and Weedon, G. P.: A global water resources ensemble of hydrological models: the earth2Observe Tier-1 dataset, *Earth Syst. Sci. Data*, 9, 389–413, <https://doi.org/10.5194/essd-9-389-2017>, 2017.

Schwanghart, W., and Kuhn, N. J.: TopoToolbox: A set of Matlab functions for topographic analysis., *Environ. Model. Softw. Environmental Modelling & Software*, 25(6), 770–781, 2010.

Seneviratne, S. I., Corti, T., Davin, E. L., Hirschi, M., Jaeger, E. B., Lehner, I., ... and Teuling, A. J.: Investigating soil moisture–climate interactions in a changing climate: A review, *Earth-Sci. Rev.*, 99(3-4), 125-161, <https://doi.org/10.1016/j.earscirev.2010.02.004>, 2010.

Sneeuw, N., Lorenz, C., Devaraju, B., Tourian, M. J., Riegger, J., Kunstmann, H., and Bárdossy, A.: Estimating runoff using hydro-geodetic approaches, *Surv. Geophys.*, 35(6), 1333-1359, <https://doi.org/10.1007/s10712-014-9300-4>, 2014.

Solomatine, D. P., and Ostfeld, A.: Data-driven modelling: some past experiences and new approaches, *J. Hydroinform.*, 10(1), 3-22, <https://doi.org/10.2166/hydro.2008.015>, 2008.

Strahler, A. N.: Hypsometric (area-altitude) analysis of erosional topography, *Geol. Soc. Am. Bull.*, Geological Society of America Bulletin, 63(11), 1117-1142, [https://doi.org/10.1130/0016-7606\(1952\)63\[1117:HAAOET\]2.0.CO;2](https://doi.org/10.1130/0016-7606(1952)63[1117:HAAOET]2.0.CO;2), 1952.

Tapley, B.D., Watkins, M.M., Flechtner, F. et al.: Contributions of GRACE to understanding climate change, *Nat. Clim. Chang.*, 9, 358–369, <https://doi.org/doi:10.1038/s41558-019-0456-2>, 2019.

Thiemig, V., Rojas, R., Zambrano-Bigiarini, M., and De Roo, A.: Hydrological evaluation of satellite rainfall estimates over the Volta and Baro-Akobo Basin, *J. Hydrol.*, 499, 324-338, <https://doi.org/10.1016/j.jhydrol.2013.07.012>, 2013.

Tourian, M. J., Reager, J. T., and Sneeuw, N.: The total drainable water storage of the Amazon river basin: A first estimate using GRACE, *Water Resour. Res.*, 54, <https://doi.org/10.1029/2017WR021674>, 2018.

Tramblay, Y., Bouvier, C., Martin, C., Didon-Lescot, J. F., Todorovik, D., and Domergue, J. M.: Assessment of initial soil moisture conditions for event-based rainfall–runoff modelling, *J. Hydrol.*, 387(3-4), 176-187, <https://doi.org/10.1016/j.jhydrol.2010.04.006>, 2010.

Troutman, B. M., and Karlinger, M.B.: Unit hydrograph approximation assuming linear flow through topologically random channel networks, *Water Resour. Res.*, 21, 743 – 754, <https://doi.org/doi:10.1029/WR021i005p00743>, 1985.

Vörösmarty C. J., and Coauthors: Global water data: A newly endangered species, *Eos, Trans. Amer. Geophys. Union.*, 82, 54, <https://doi.org/10.1029/01EO00031>, 2002.

Vose, R.S., Applequist, S., Durre, I., Menne, M.J., Williams, C.N., Fenimore, C., Gleason, K., and Arndt, D.: Improved Historical Temperature and Precipitation on Time Series For U.S. Climate Divisions., *J. Meteorol. and Climat.*, 53(May), 1232–1251., <https://doi.org/10.1175/JAMC-D-13-0248.1> DOI: 10.1175/JAMC-D-13-0248.1, 2014.

Wagner, W., Blöschl, G., Pampaloni, P., Calvet, J. C., Bizzarri, B., Wigneron, J. P., and Kerr, Y.: Operational readiness of microwave remote sensing of soil moisture for hydrologic applications, *Hydrol. Res.*, 38(1), 1-20, <https://doi.org/10.2166/nh.2007.029>, 2007.

Wagner, W., Lemoine, G., and Rott, H.: A method for estimating soil moisture from ERS scatterometer and soil data., *Remote Sens. Environ.*, Remote Sensing of Environment, 70, 191–207, [https://doi.org/doi:10.1016/S0034-4257\(99\)00036-X](https://doi.org/doi:10.1016/S0034-4257(99)00036-X), 1999.

Wisser, D., Fekete, B. M., Vörösmarty, C. J., and Schumann, A. H.: Reconstructing 20th century global hydrography: a contribution to the Global Terrestrial Network- Hydrology (GTN-H), *Hydrol. Earth Syst. Sci.*, 14, 1–24, <https://doi.org/doi:10.5194/hess-14-1-2010>, 2010.

Yokoo, Y., and Sivapalan, M.: Towards reconstruction of the flow duration curve: Development of a conceptual framework with a physical basis, *Hydrol. Earth Syst. Sci.*, 15(9), 2805–2819, <https://doi.org/10.5194/hess-15-2805-2011>, 2011.

Zhang, Y., Pan, M., Sheffield, J., Siemann, A. L., Fisher, C. K., Liang, M., ... and Zhou, T.: A Climate Data Record (CDR) for the global terrestrial water budget: 1984–2010, *Hydrol. Earth Syst. Sci.*, 22, 241–263, [https://doi.org/10.5194/hess-22-241-2018\(Online\)](https://doi.org/10.5194/hess-22-241-2018(Online)), 22(PNNL-SA-129750), 2018.

Albergel, C., Rüdiger, C., Carrer, D., Calvet, J. C., Fritz, N., Naeimi, V., Bartalis, Z., & Hasenauer, S. (2009). An evaluation of ASCAT surface soil moisture products with in-situ observations in southwestern France. *Hydrology and Earth System Sciences*, 13, 115–124, doi:10.5194/hess-13-115-2009.

Allen RG, Pereira LS, Raes D, Smith M (1998) Crop evapotranspiration — guidelines for computing crop water requirements. FAO Irrigation & Drainage Paper 56. FAO, Rome.



Balsamo, G., A. Beljaars, K. Scipal, P. Viterbo, B. vanden Hurk, M. Hirschi, and A. K. Betts (2009). A revised hydrology for the ECMWF model: Verification from field site to terrestrial water storage and impact in the integrated forecast system, *J. Hydrometeorol.*, 10(3), 623–643.

Barbarossa, V., Huijbregts, M. A., Beusen, A. H., Beck, H. E., King, H., & Schipper, A. M. (2018). FLO1K, global maps of mean, maximum and minimum annual streamflow at 1 km resolution from 1960 through 2015. *Scientific data*, 5, 180052.

Beck, H. E., van Dijk, A. I., de Roo, A., Dutra, E., Fink, G., Orth, R., & Schellekens, J. (2017). Global evaluation of runoff from ten state-of-the-art hydrological models. *Hydrology and Earth System Sciences*, 21(6), 2881–2903. doi:doi.org/10.5194/hess-21-2881-2017.

Berghuijs, W. R., Woods, R. A., Hutton, C. J., and Sivapalan, M. (2016). Dominant flood-generating mechanisms across the United States, *Geophys. Res. Lett.*, 43, 4382–4390.

Berthet, L., Andréassian, V., Perrin, C., & Javelle, P. (2009). How crucial is it to account for the antecedent moisture conditions in flood forecasting? Comparison of event-based and continuous approaches on 178 catchments. *Hydrology and Earth System Sciences*, 13(6), 819–831.

Blöschl, G., Sivapalan, M., Wagener, T., Viglione, A., & Savenije, H. H. G. (Eds.) (2013). *Runoff predictions in ungauged basins: A synthesis across processes, places and scales*. Cambridge: Cambridge University Press.

Botter, G., Porporato, A., Daly, E., Rodriguez-Iturbe, I., and Rinaldo, A. (2007a). Probabilistic characterization of base flows in river basins: Roles of soil, vegetation, and geomorphology. *Water Resour. Res.*, 43, W06404. doi:10.1029/2006WR005397.

Botter, G., Peratoner, F., Porporato, A., Rodriguez-Iturbe, I., and Rinaldo, A. (2007b). Signatures of large-scale soil moisture dynamics on streamflow statistics across U.S. Climate regimes. *Water Resour. Res.*, 43, W11413, doi:10.1029/2007WR006162.

Botter, G., Porporato, A., Daly, E., Rodriguez-Iturbe, I., and Rinaldo, A. (2007a). Probabilistic characterization of base flows in river basins: Roles of soil, vegetation, and geomorphology. *Water Resour. Res.*, 43, W06404. doi:10.1029/2006WR005397.

Brocca, L., Melone, F., Moramarco, T. (2008). On the estimation of antecedent wetness conditions in rainfall-runoff modelling. *Hydrological Processes*, 22 (5), 629–642, doi:10.1002/hyp.6629.

Brocca, L., Melone, F., Moramarco, T., & Morbidelli, R. (2009). Antecedent wetness conditions based on ERS scatterometer data. *Journal of Hydrology*, 364(1–2), 73–87.

Brocca, L., Melone, F., & Moramarco, T. (2011). Distributed rainfall-runoff modelling for flood frequency estimation and flood forecasting. *Hydrological processes*, 25(18), 2801–2813.

Brocca, L., Ciabatta, L., Massari, C., Camici, S., & Tarpanelli, A. (2017). Soil moisture for hydrological applications: open questions and new opportunities. *Water*, 9(2), 140.

Cai, X., Yang, Z. L., David, C. H., Niu, G. Y., & Rodell, M. (2014). Hydrological evaluation of the Noah-MP land surface model for the Mississippi River Basin. *Journal of Geophysical Research: Atmospheres*, 119(1), 23–38.

Cislaghi, A., Masseroni, D., Massari, C., Camici, S., & Brocca, L. (2020). Combining a rainfall-runoff model and a regionalization approach for flood and water resource assessment in the western Po Valley, Italy. *Hydrological Sciences Journal*, 65(3), 348–370.

Crochemore, L., Isberg, K., Pimentel, R., Pineda, L., Hasan, A., & Arheimer, B. (2020). Lessons learnt from checking the quality of openly accessible river flow data worldwide. *Hydrological Sciences Journal*, 65(5), 699–711.

Crow, W. T., Bindlish, R., & Jackson, T. J. (2005). The added value of spaceborne passive microwave soil moisture retrievals for forecasting rainfall-runoff partitioning. *Geophysical Research Letters*, 32(18).

Döll, P., F. Kaspar, and B. Lehner (2003). A global hydrological model for deriving water availability indicators: Model tuning and validation, *J. Hydrol.*, 270(1–2), 105–134, doi:10.1016/S0022-1694(02)00283-4.

Dorigo, W., Wagner, W., Albergel, C., Albrecht, F., Balsamo, G., Brocca, L., Chung, D., Ertl, M., Forkel, M., Gruber, A., Haas, D., Hamer, P., Hirschi, M., Ikonen, J., de Jeu, R., Kidd, R., Lahoz, W., Liu, Y. Y., Miralles, D., Mistelbauer, T., Nicolai-Shaw, N., Parinussa, R., Pratola, C., Reimer, C., van der Schalie, R., Seneviratne, S. I., Smolander, T.,

**Formattato:** Tipo di carattere: Non Corsivo

**Formattato:** Inglese (Regno Unito)

932 Lecomte, P. (2017). ESA CCI Soil Moisture for improved Earth-system understanding: state-of-the-art and future  
 933 directions. *Remote Sensing of Environment*, 203, 185–215.

934 Entekhabi, D., Njoku, E. G., O'Neill, P. E., Kellogg, K. H., Crow, W. T., Edelstein, W. N., ... & Van Zyl, J. (2010). The  
 935 soil moisture active passive (SMAP) mission. *Proceedings of the IEEE*, 98(5), 704–716. doi:  
 936 10.1109/JPROC.2010.2043918.

937 Famiglietti, J. S., Wood, E. F. (1994). Multiscale modeling of spatially variable water and energy balance processes. *Water*  
 938 *Resour. Res.*, 30, 3061–3078.

939 Famiglietti, J. S., & Rodell, M. (2013). Water in the balance. *Science*, 340(6138), 1300–1301.

940 Fan, Y., & Van den Dool, H. A. (2008). Global monthly land surface air temperature analysis for 1948–present. *Journal of*  
 941 *Geophysical Research: Atmospheres* 113, D01103.

942 Fekete, B. M., Looser, U., Pietroniro, A., and Robarts, R. D. (2012). Rationale for monitoring discharge on the ground,  
 943 *J. Hydrometeorol.*, 13, 1977–1986.

944 Georgakakos KP, Baumer OW. (1996). Measurement and utilization of onsite soil moisture data. *Journal of Hydrology*  
 945 184: 131–152.

946 Ghiggi, G., Humphrey, V., Seneviratne, S. I., & Gudmundsson, L. (2019). GRUN: an observation-based global gridded  
 947 runoff dataset from 1902 to 2014. *Earth System Science Data*, 11(4), 1655–1674.

948 Ghotbi, S., Wang, D., Singh, A., Blöschl, G., & Sivapalan, M. (2020). A New Framework for Exploring Process Controls  
 949 of Flow Duration Curves. *Water Resources Research*, 56(1), e2019WR026083.

950 Gudmundsson, L., & Seneviratne, S. I. (2016). Observation-based gridded runoff estimates for Europe (E-RUN version  
 951 1.1). *Earth System Science Data*, 8(2), 279–295.

952 Gudmundsson, L., Wagener, T., Tallaksen, L. M., & Engeland, K. (2012a). Evaluation of nine large-scale hydrological  
 953 models with respect to the seasonal runoff climatology in Europe. *Water Resources Research*, 48(11).

954 Gudmundsson, L., Tallaksen, L. M., Stahl, K., Clark, D. B., Du-mont, E., Hagemann, S., Bertrand, N., Gerten, D., Heinke,  
 955 J., Hanasaki, N., Voss, F., and Koirala, S. (2012b). Comparing Large-Scale Hydrological Model Simulations to  
 956 Observed Runoff Percentiles in Europe, *J. Hydrometeorol.*, 13, 604–62.

957 Gupta-VK, Waymire E, Wang CT. (1980). A representation of an instantaneous unit hydrograph from geomorphology.  
 958 *Water Resources Research* 16: 855–862, doi: 10.1029/WR016i005p00855.

959 Gupta, H. V., Kling, H., Yilmaz, K. K., & Martinez, G. F. (2009). Decomposition of the mean squared error and NSE  
 960 performance criteria: Implications for improving hydrological modelling. *Journal of Hydrology*, 377(1–2), 80–91.

961 Haddeland, I., Heinke, J., Voß, F., Eisner, S., Chen, C., Hagemann, S., & Ludwig, F. (2012). Effects of climate model  
 962 radiation, humidity and wind estimates on hydrological simulations. *Hydrology and Earth System Sciences*, 16(2),  
 963 305–318.

964 Hastie, T., Tibshirani, R., and Friedman, J. H. (2009). *The Elements of Statistical Learning—Data Mining, Inference, and*  
 965 *Prediction*, Second Edition, Springer Series in Statistics, Springer, New York, 2nd Edn., available at:

966 Hong, Y., Adler, R. F., Hossain, F., Curtis, S., & Huffman, G. J. (2007). A first approach to global runoff simulation  
 967 using satellite rainfall estimation. *Water Resources Research*, 43(8).

968 Horton, R. E. (1945). Hydrological approach to quantitative morphology. *Geol. Soc. Am. Bull.*, 56, 275–370.

969 Houborg, R., Rodell, M., Li, B., Reichle, R., & Zaitchik, B. F. (2012). Drought indicators based on model-assimilated  
 970 Gravity Recovery and Climate Experiment (GRACE) terrestrial water storage observations. *Water Resources*  
 971 *Research*, 48(7).

972 Hu GR., Li XY. (2018). Subsurface Flow. In: Li X., Vereecken H. (eds) *Observation and Measurement*. *Ecohydrology*.  
 973 Springer, Berlin, Heidelberg.

974 Huffman, G. J., R. F. Adler, D. T. Bolvin, G. J. Gu, E. J. Nelkin, K. P. Bowman, Y. Hong, E. F. Stocker, and D. B. Wolff.  
 975 (2007). The TRMM Multisatellite Precipitation Analysis (TMPA): Quasi-Global, Multiyear, Combined Sensor  
 976 Precipitation Estimates at Fine Scales. *Journal of Hydrometeorology* 8 (1): 38–55. doi:10.1175/jhm560.1.

Formattato: Inglese (Regno Unito)

Huffman, G. J., Stocker, E. F., Bolvin, D. T., Nelkin, E. J., & Adler, R. F. (2014). TRMM Version 7 3B42 and 3B43 Data Sets. NASA/GSFC, Greenbelt, MD.

Huffman, G. J., Bolvin, D. T., Braithwaite D., Hsu K., Joyce R., Kidd C., Nelkin Eric J., Sorooshian S., Tan J., Xie P. (2019). NASA Global Precipitation Measurement (GPM) Integrated Multi-satellite Retrievals for GPM (IMERG).

Kim, H., Watanabe, S., Chang, E. C., Yoshimura, K., Hirabayashi, J., Famiglietti, J., and Oki, T. (2017). Global Soil Wetness Project Phase 3 Atmospheric Boundary Conditions (Experiment 1) [Data set], Data Integration and Analysis System (DIAS).

Kirchner, J. W. (2006). Getting the right answers for the right reasons: Linking measurements, analyses, and models to advance the science of hydrology. *Water Resources Research*, 42(3).

Kling, H., Fuchs, M., & Paulin, M. (2012). Runoff conditions in the upper Danube basin under an ensemble of climate change scenarios. *Journal of Hydrology*, 424, 264–277. doi: 10.1016/j.jhydrol.2012.01.011.

Landerer, F. W., & Swenson, S. C. (2012). Accuracy of scaled GRACE terrestrial water storage estimates. *Water resources research*, 48(4).

Lehner, B., C. Reidy Liermann, C. Revenga, C. Vörösmarty, B. Fekete, P. Crouzet, P. Döll, M. Endejan, K. Frenken, J. Magome, C. Nilsson, J.C. Robertson, R. Rodel, N. Sindorf, and D. Wisser. 2011. High-resolution mapping of the world's reservoirs and dams for sustainable river-flow management. *Frontiers in Ecology and the Environment* 9 (9): 494–502.

Long, D., Longuevergne, L., & Scanlon, B. R. (2014). Uncertainty in evapotranspiration from land surface modeling, remote sensing, and GRACE satellites. *Water Resources Research*, 50(2), 1131–1151.

Lorenz, C., H. Kunstmann, B. Devaraju, M. J. Tourian, M. J. N. Sneeuw, and J. Riegger (2014). Large-Scale Runoff from Landmasses: A Global Assessment of the Closure of the Hydrological and Atmospheric Water Balances. *J. Hydrometeor.*, 15, 2111–2139. doi:10.1175/JHM-D-13-0157.1.

Lutheke, S.B., Sabaka, T.J., Loomis, B.D., Arendt, A.A., McCarthy, J.J., Camp, J. (2013) Antarctica, Greenland and Gulf of Alaska land-ice evolution from an iterated GRACE global mascon solution, *Journal of Glaciology*, Vol. 59, No. 216, 2013.

Massari, C., Brocca, L., Tarpanelli, A., Hong, Y., Crow, W., Ciabatta, L., Camici, S., Barbeta, S., Moramarco, T. (2016). Global surface runoff estimation in near real time by using SMAP and GPM, poster at SMAP conference.

Massari, C., Brocca, L., Barbeta, S., Papathanasiou, C., Mimikou, M., & Moramarco, T. (2014). Using globally available soil moisture indicators for flood modelling in Mediterranean catchments. *Hydrology and Earth System Sciences*, 18(2), 839.

Merz, R., & Blöschl, G. (2009). A regional analysis of event runoff coefficients with respect to climate and catchment characteristics in Austria. *Water Resources Research*, 45(1).

Mueller Schmied, H., Adam, L., Eisner, S., Fink, G., Flörke, M., Kim, H., ... & Song, Q. (2016). Variations of global and continental water balance components as impacted by climate forcing uncertainty and human water use. *Hydrology and Earth System Sciences*, 20(7), 2877–2898.

Muneepeerakul, R., Azalee, S., Botter, G., Rinaldo, A., & Rodriguez-Iturbe, I. (2010). Daily streamflow analysis based on a two-scaled gamma pulse model. *Water Resources Research*, 46(11).

Nash, J. E. (1957). The form of the instantaneous unit hydrograph, IASH publication no. 45, 3–4, 114–121.

Natural Resources Conservation Service (NRCS) (1986). Urban hydrology for small watersheds, Tech. Release 55, 2nd ed., U.S. Dep. of Agric., Washington, D. C. (available at [ftp://ftp.wcc.nrcs.usda.gov/downloads/hydrology\\_hydraulics/tr55/tr55.pdf](ftp://ftp.wcc.nrcs.usda.gov/downloads/hydrology_hydraulics/tr55/tr55.pdf))

Orth, R., & Seneviratne, S. I. (2015). Introduction of a simple model based land surface dataset for Europe. *Environmental Research Letters*, 10(4), 044012.

Pellet, V., Aires, F., Munier, S., Fernández Prieto, D., Jordá, G., Dorigo, W. A., ... & Brocca, L. (2019). Integrating multiple satellite observations into a coherent dataset to monitor the full water cycle—application to the Mediterranean region. *Hydrology and Earth System Sciences*, 23(1), 465–491.

Formattato: Inglese (Regno Unito)

Formattato: Inglese (Regno Unito)

1023 Prudhomme, C., Giuntoli, I., Robinson, E. L., Clark, D. B., Arnell, N. W., Dankers, R., ... & Hagemann, S. (2014).  
1024 Hydrological droughts in the 21st century, hotspots and uncertainties from a global multimodel ensemble experiment.  
1025 *Proceedings of the National Academy of Sciences*, 111(9), 3262–3267.

1026 Rakovec, O., Kumar, R., Attinger, S., & Samaniego, L. (2016). Improving the realism of hydrologic model functioning  
1027 through multivariate parameter estimation. *Water Resources Research*, 52(10), 7779–7792.

1028 Richards, L.A. (1931). Capillary conduction of liquids through porous mediums. *Physics*, 1 (5): 318–333.  
1029 Bibcode:1931Physi.1.318R. doi:10.1063/1.1745010.

1030 Riegger, J., and M. J. Tourian M. J. (2014). Characterization of runoff storage relationships by satellite gravimetry and  
1031 remote sensing. *Water Resour. Res.*, 50, 3444–3466, doi:10.1002/2013WR013847.

1032 Rodell, M., Beaudoing, H. K., L'Ecuyer, T. S., Olson, W. S., Famiglietti, J. S., Houser, P. R., Adler, R., Bosilovich, M.  
1033 G., Clayson, C. A., Chambers, D., Clark, E., Fetzner, E. J., Gao, X., Gu, G., Hilburn, K., Huffman, G. J., Lettenmaier,  
1034 D. P., Liu, W. T., Robertson, F. R., Schlosser, C. A., Sheffield, J. and Wood, E. F. (2015). The observed state of the  
1035 water cycle in the early 15twenty first century. *J. Clim.*, 28(21), 8289–8318,.

1036 Schellekens, J., Dutra, E., Martínez-de la Torre, A., Balsamo, G., van Dijk, A., Sperna-Weiland, F., Minvielle, M., Cal-  
1037 vet, J. C., Decharme, B., Eisner, S., Fink, G., Flörke, M., Peßenteiner, S., van Beek, R., Polcher, J., Beck, H., Orth, R.,  
1038 Calton, B., Burke, S., Dorigo, W., and Weedon, G. P. (2017). A global water resources ensemble of hydrological  
1039 models: the earthH2Observe Tier 1 dataset. *Earth Syst. Sci. Data*, 9, 389–413, <https://doi.org/10.5194/essd-9-389-2017>.

1040 Schwanhart, W., & Kuhn, N. J. (2010). TopoToolbox: A set of Matlab functions for topographic analysis. *Environmental*  
1041 *Modelling & Software*, 25(6), 770–781.

1042 Seneviratne, S. I., Corti, T., Davin, E. L., Hirschi, M., Jaeger, E. B., Lehner, I., ... & Teuling, A. J. (2010). Investigating  
1043 soil moisture–climate interactions in a changing climate: A review. *Earth Science Reviews*, 99(3–4), 125–161.

1044 Sneeuw, N., Lorenz, C., Devaraju, B., Tourian, M. J., Riegger, J., Kunstmann, H., & Bárdossy, A. (2014). Estimating  
1045 runoff using hydro-geodetic approaches. *Surveys in Geophysics*, 35(6), 1333–1359.

1046 Solomatine, D. P., & Ostfeld, A. (2008). Data-driven modelling: some past experiences and new approaches. *Journal of*  
1047 *hydroinformatics*, 10(1), 3–22.

1048 Strahler, A. N. (1952). Hypsometric (area-altitude) analysis of erosional topography. *Geological Society of America*  
1049 *Bulletin*, 63(11), 1117–1142.

1050 Tapley, B.D., Watkins, M.M., Flechtner, F. et al. (2019). Contributions of GRACE to understanding climate change. *Nat.*  
1051 *Clim. Chang.* 9, 358–369,.

1052 Thiemeig, V., Rojas, R., Zambrano Bigiarini, M., & De Roo, A. (2013). Hydrological evaluation of satellite rainfall  
1053 estimates over the Volta and Baro-Akobo Basin. *Journal of Hydrology*, 499, 324–338.

1054 Tourian, M. J., Reager, J. T., & Sneeuw, N. (2018). The total drainable water storage of the Amazon river basin: A first  
1055 estimate using GRACE. *Water Resources Research*, 54,.

1056 Trambly, Y., Bouvier, C., Martin, C., Didon-Lescot, J. F., Todorovik, D., & Domergue, J. M. (2010). Assessment of  
1057 initial soil moisture conditions for event-based rainfall-runoff modelling. *Journal of Hydrology*, 387(3–4), 176–187.

1058 Troutman, B. M., Karlinger, M.B. (1985). Unit hydrograph approximation assuming linear flow through topologically  
1059 random channel networks. *Water Resources Research*, 21: 743–754,.

1060 Vose, R.S., Applequist, S., Durre, I., Menne, M.J., Williams, C.N., Fenimore, C., Gleason, K., & Arndt, D. (2014).  
1061 Improved Historical Temperature and Precipitation Time Series For U.S. Climate Divisions. *Journal of Applied*  
1062 *Meteorology and Climatology*, 53(May), 1232–1251. DOI: 10.1175/JAMC-D-13-0248.1

1063 Vörösmarty C. J., and Coauthors (2002). Global water data: A newly endangered species. *Eos, Trans. Amer. Geophys.*  
1064 *Union*, 82, 54.

1065 Wagner, W., Blöschl, G., Pampaloni, P., Calvet, J. C., Bizzarri, B., Wigneron, J. P., & Kerr, Y. (2007). Operational  
1066 readiness of microwave remote sensing of soil moisture for hydrologic applications. *Hydrology Research*, 38(1), 1–  
1067 20.

1068 Wagner, W., Lemoine, G., & Rott, H. (1999). A method for estimating soil moisture from ERS scatterometer and soil  
1069 data. *Remote Sensing of Environment*, 70, 191–207,.

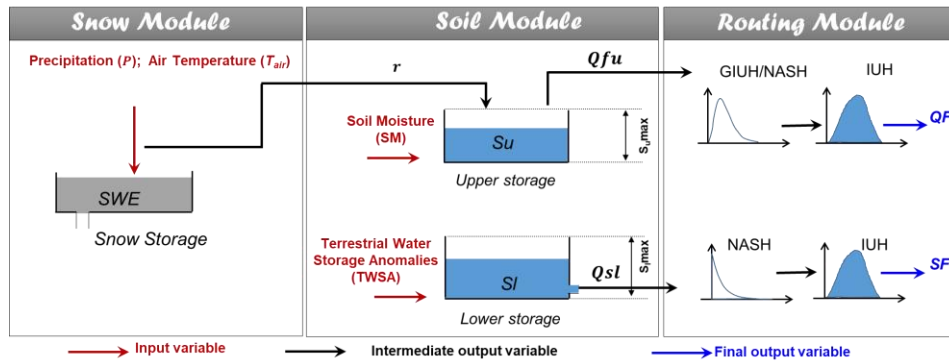
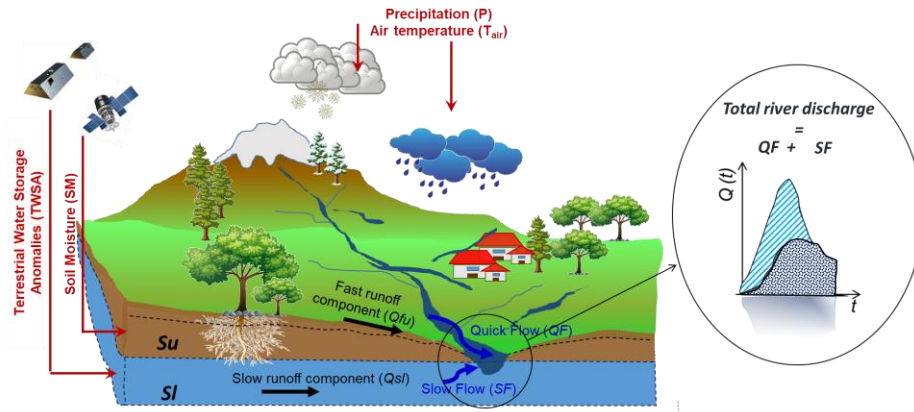
- Wisser, D., Fekete, B. M., Vörösmarty, C. J., and Schumann, A. H. (2010). Reconstructing 20th-century global hydrography: a contribution to the Global Terrestrial Network–Hydrology (GTN-H), *Hydrol. Earth Syst. Sci.*, 14, 1–24.
- Yokoo, Y., & Sivapalan, M. (2011). Towards reconstruction of the flow duration curve: Development of a conceptual framework with a physical basis. *Hydrology and Earth System Sciences*, 15(9), 2805–2819. <https://doi.org/10.5194/hess-15-2805-2011>.
- Zhang, Y., Pan, M., Sheffield, J., Siemann, A. L., Fisher, C. K., Liang, M., ... & Zhou, T. (2018). A Climate Data Record (CDR) for the global terrestrial water budget: 1984–2010. *Hydrology and Earth System Sciences (Online)*, 22(PNPL-SA-129750).

Table 1. Location of gauging stations over the Mississippi basins and upstream contributing area. Bold text is used to indicate stations where the STREAM v1.3 model has been calibrated.

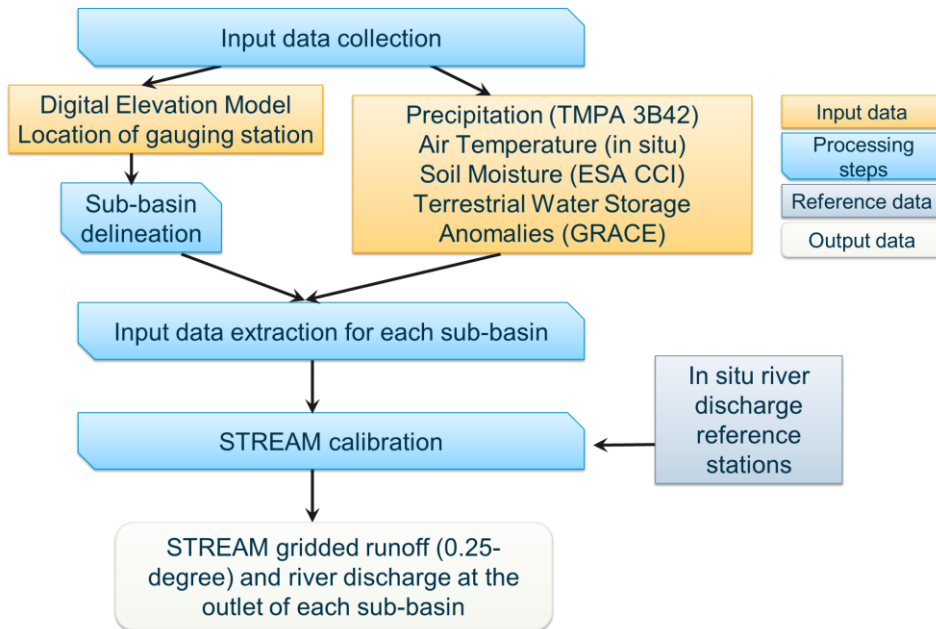
#	River	Station name	Latitude (°)	Longitude (°)	Upstream area (km <sup>2</sup> )	Mean annual river discharge (m <sup>3</sup> /s)	Presence of dam
1	Missouri	Bismarck, ND	-100.82	46.81	481'232	633	Garrison dam
2	Missouri	Omaha, NE	-95.92	41.26	814'371	914	Gavins Point Dam
3	Missouri	Kansas City, MO	-94.59	39.11	1'229'427	1499	---
4	Missouri	<b>Hermann, MO</b>	<b>-91.44</b>	<b>38.71</b>	<b>1'330'000</b>	<b>2326</b>	---
5	Kansas	Wamego, KS	-96.30	39.20	143'054	141	Kanopolis
6	Mississippi	<b>Keokuk, IA</b>	<b>-91.37</b>	<b>40.39</b>	<b>282'559</b>	<b>1948</b>	---
7	Rock	Near Joslin, IL	-90.18	41.56	23'835	199	---
8	Mississippi	Chester, IL	-89.84	37.90	1'776'221	6018	---
9	Arkansas	<b>Murray Dam Near Little Rock, AR</b>	<b>-92.36</b>	<b>34.79</b>	<b>408'068</b>	<b>1249</b>	---
10	Mississippi	<b>Vicksburg, MS</b>	<b>-90.91</b>	<b>32.32</b>	<b>2'866'590</b>	<b>17487</b>	---
11	Ohio	<b>Metropolis, ILL.</b>	<b>-88.74</b>	<b>37.15</b>	<b>496'134</b>	<b>7931</b>	---

1084 Table 2. Performance scores obtained over the Mississippi river sections during the calibration and  
1085 validation periods.

#	CALIBRATION PERIOD			VALIDATION PERIOD		
SCORE	KGE (-)	R (-)	RRMSE (%)	KGE (-)	R (-)	RRMSE (%)
CALIBRATED SECTIONS						
10	0.78	0.78	30	0.74	0.80	38
9	0.62	0.75	71	0.67	0.85	77
6	0.83	0.84	39	0.73	0.84	46
4	0.77	0.78	46	0.72	0.75	50
11	0.82	0.82	44	0.70	0.86	51
SECTIONS NOT USED FOR CALIBRATION						
1	-3.26	0.08	137	0.20	0.44	96
2	-0.57	0.48	118	0.40	0.53	89
3	0.16	0.71	83	0.39	0.70	72
5	-1.49	0.24	368	-1.26	0.31	358
7	0.53	0.68	71	0.20	0.70	81
8	0.80	0.84	36	0.77	0.84	39



1097



1098

1099

1100 Figure 2. Processing steps of the STREAM v1.3 model.

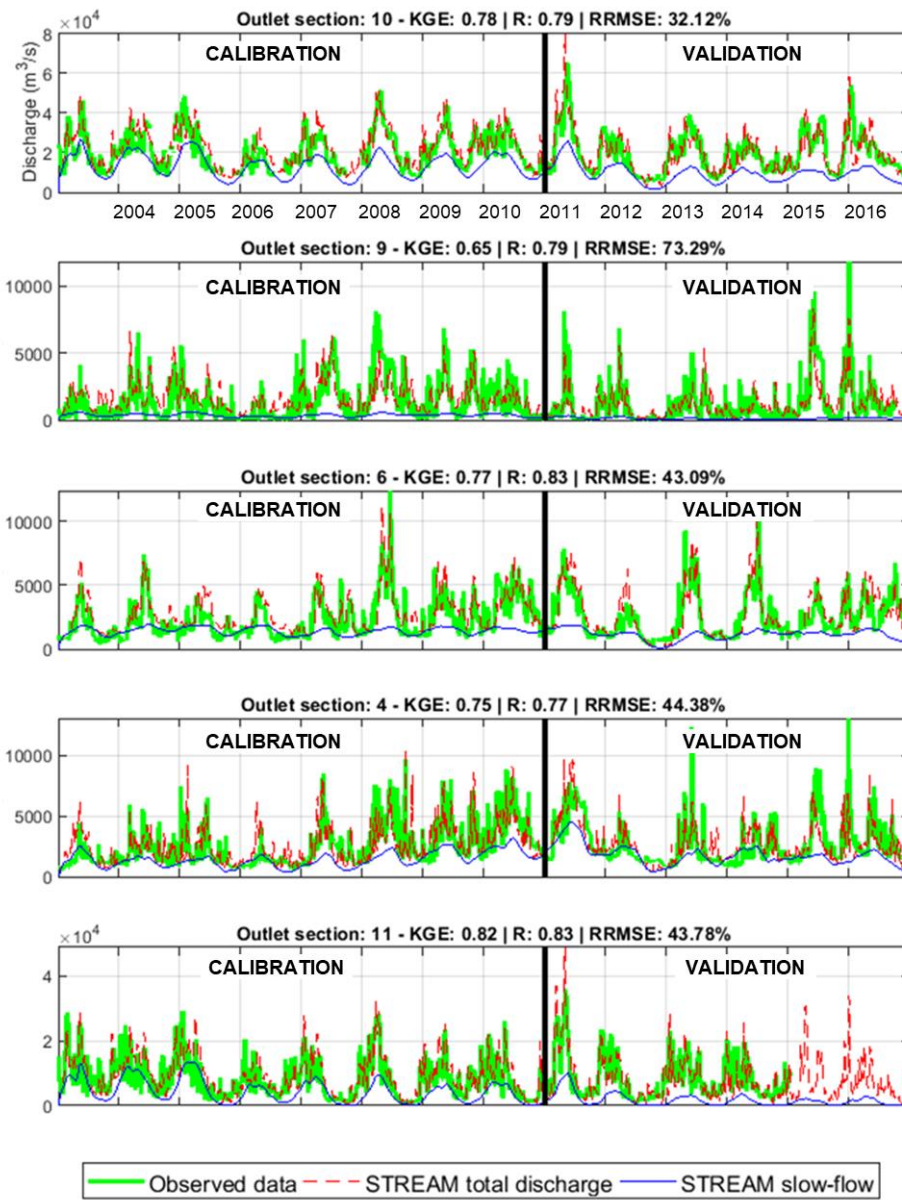
1101

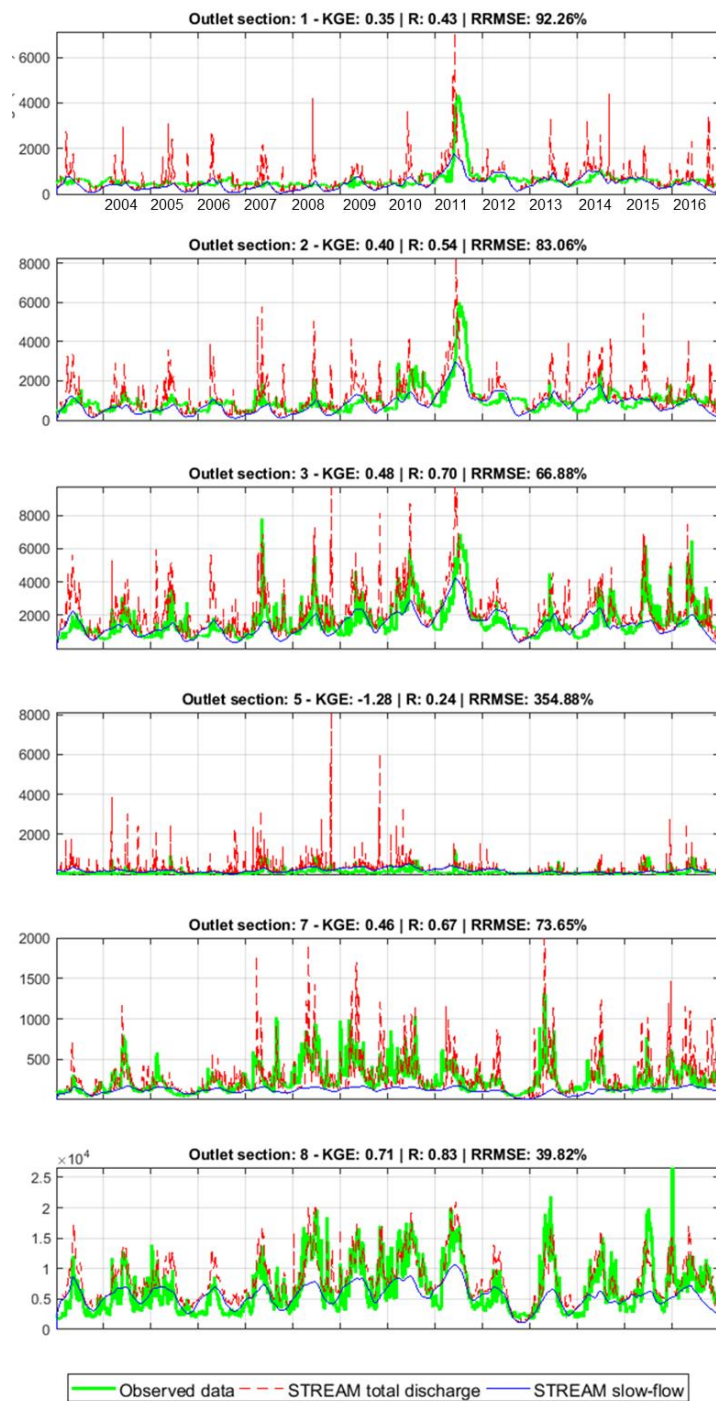


1104

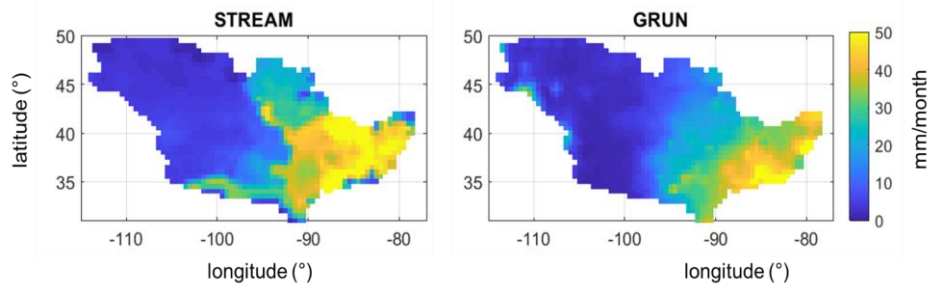


1105 Figure 3. Mississippi sub-basin delineation. Red dots indicate the location of the discharge gauging  
1106 stations; different colours identify different inner sections (and the related contributing sub-basins)  
1107 used for the model calibration.  
1108





1116  
1117 Figure 5. Comparison between observed and simulated river discharge time series over the gauged  
1118 sections not used in the calibration phase. Performance scores at the top of each plot refer to the entire  
1119 study period (2003–2016).  
1120



1121

1122 Figure 6. Mississippi river basin: mean monthly runoff for the period 2003–2014 obtained by  
1123 STREAM v1.3 and GRUN models.  
1124

1125    **APPENDIX**

1126    Table 1A. Description of STREAM v1.3 parameters, belonging module, variability range and unit.

Parameter	Description	Module	Range Variability	Unit
Cm	degree-day coefficient	Snow	0.1/24-3	[-]
$\alpha$	exponent of infiltration	Soil	1-30	[-]
T	characteristic time length	Soil	0.01-80	[days]
$\beta$	coefficient relationship slow runoff component and TWSA	Soil	0.1-20	[mm h-1]
m	exponent in the relationship between slow runoff component and TWSA	Soil	1-15	[-]
$\gamma$	parameter of GIUH	Routing	0.5-5.5	[-]
C	Celerity	Routing	1-60	[km h-1]
D	Diffusivity	Routing	1-30	[km2 h-1]

1127